Protein Lysine Methyltransferase G9a Inhibitors: Design, Synthesis, and Structure Activity Relationships of 2,4-Diamino-7-aminoalkoxy-quinazolines.[†]

Feng Liu,[‡] Xin Chen,[‡] Abdellah Allali-Hassani,[§] Amy M. Quinn,[||] Tim J. Wigle,[‡] Gregory A. Wasney,[§] Aiping Dong,[§] Guillermo Senisterra,[§] Irene Chau,[§] Alena Siarheyeva,[§] Jacqueline L. Norris,[‡] Dmitri B. Kireev,[‡] Ajit Jadhav,[||] J. Martin Herold,[‡] William P. Janzen,[‡] Cheryl H. Arrowsmith,[§] Stephen V. Frye,[‡] Peter J. Brown,[§] Anton Simeonov,[||] Masoud Vedadi,[§] and Jian Jin*,[‡]

[‡]*Center for Integrative Chemical Biology and Drug Discovery, Division of Medicinal Chemistry and Natural Products, Eshelman School of Pharmacy, University of North Carolina at Chapel Hill, Chapel Hill, North Carolina 27599,* [§]*Structural Genomics Consortium, University of Toronto, Toronto, Ontario M5G 1L7, Canada, and* [||]*NIH Chemical Genomics Center, National Human Genome Research Institute, National Institutes of Health, Bethesda, Maryland 20892*

Protein lysine methyltransferase G9a, which catalyzes methylation of lysine 9 of histone H3 (H3K9) and lysine 373 (K373) of p53, is overexpressed in human cancers. Genetic knockdown of G9a inhibits cancer cell growth, and the dimethylation of p53 K373 results in the inactivation of p53. Initial SAR exploration of the 2,4-diamino-6,7-dimethoxyquinazoline template represented by **3a** (BIX01294), a selective small molecule inhibitor of G9a and GLP, led to the discovery of **10** (UNC0224) as a potent G9a inhibitor with excellent selectivity. A high resolution X-ray crystal structure of the G9a−**10** complex, the first cocrystal structure of G9a with a small molecule inhibitor, was obtained. On the basis of the structural insights revealed by this cocrystal structure, optimization of the 7-dimethylaminopropoxy side chain of **10** resulted in the discovery of **29** (UNC0321) (Morrison $K_i = 63$ pM), which is the first G9a inhibitor with picomolar potency and the most potent G9a inhibitor to date.

Introduction

Epigenetics is defined as changes in gene function that are mitotically and/or meiotically heritable and that do not entail a change in DNA sequence. Over the past decade, the cellular machinery that creates these heritable changes has been intensely investigated by the biomedical research community as there is no area of biology, or for that matter no area of human health, where epigenetics may not play a fundamental role.[1] The template upon which the epigenome is written is chromatin that is primarily made up of DNA wrapped around octamers of histone proteins. The state of chromatin, and therefore access to the genetic code, is mainly regulated by covalent and reversible PTMs to histones and DNA, and the recognition of these marks by other proteins and protein complexes. The PTMs[a] of histones and DNA include: histone lysine methylation, arginine methylation,
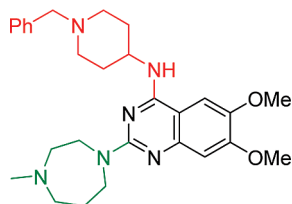
lysine acetylation, sumoylation, ADP-ribosylation, ubiquitination, glycosylation and phosphorylation, and DNA methylation.[2] Given the widespread importance of chromatin regulation to cell biology, the enzymes that produce these modifications (the "writers"), the proteins that recognize them (the "readers"), and the enzymes that remove them (the "erasers") are critical targets for manipulation to further understand the histone code[3,4] and its role in human disease. Indeed, small molecule histone deacetylase inhibitors[5] and DNA methyltransferase inhibitors[6] have already proven useful in the treatment of cancer.

Among the "writers" of the histone code, protein lysine methyltransferases (PKMTs) that catalyze mono-, di-, and/ or trimethylation of lysine residues of various proteins including histones have received great attention because of the essential function of histone lysine methylation in many biological processes including gene expression and transcriptional regulation, heterochromatin formation, and X-chromosome inactivation.[7] Since the first PKMT was characterized a decade ago,[8] more than 50 human PKMTs have been identified.[9,10] Growing evidence suggests that PKMTs play important roles in the development of various human diseases including cancer,[10−13] inflammation,[14] drug addiction,[15] mental retardation,[16] and HIV-1 latency maintenance.[17] In particular, G9a (also known as EHMT2), which was initially identified as a H3K9 methyltransferase,[18] is overexpressed in human cancers. It has been shown that knockdown of G9a inhibits cancer cell growth.[19,20] In addition to catalyzing mono- and dimethylation of H3K9, it has been shown that G9a methylates lysine 373 (K373) of p53, a tumor suppressor.[21] The dimethylation of p53 K373 results in the

Figure 1. Structure of **3a** (BIX01294).[22,29]

inactivation of p53, which is implicated in over 50% of cancers.[21] These observations suggest that inhibition of G9a is a potential approach for cancer treatment. Additionally, **3a** (BIX01294), a small molecule G9a inhibitor,[22] is efficacious as a replacement for *oct*3/4, one of the four original genetic factors used for reprogramming of mammalian somatic cells into induced pluripotent stem (iPS) cells.[23,24] Thus, small molecule PKMT inhibitors could play an important role in stem cell biology and regenerative medicine.

Despite the tremendous progress made in identifying new PKMTs and elucidating their biological function, generating small molecule PKMT inhibitors is lagging significantly behind. In fact, only two selective small molecule PKMT inhibitors (SU(VAR)3−9 inhibitor Chaetocin and G9a inhibitor **3a**)[22,25−27] have been reported since the first PKMT was characterized in 2000.[8] This gap in creating small molecule PKMT inhibitors presents a major challenge and opportunity for the biomedical research community. The creation of a "tool-kit" of potent, selective, and well-characterized chemical probes[28] of PKMTs will permit biological and therapeutic hypotheses to be tested with high confidence in cell-based and animal models of human biology and disease.

To provide potent and selective G9a inhibitors as research tools and make them available to the biomedical research community without restrictions on their use, we have explored the 2,4-diamino-6,7-dimethoxyquinazoline template represented by **3a** (Figure 1). When we began our work, this compound was the only known selective small molecule inhibitor of G9a and GLP (also known as EHMT1), which is another H3K9 and p53 K373 methyltransferase that shares 80% sequence identity with G9a in their respective SET domains.[22,29] Although **3a** was initially reported to be selective for G9a (IC$_{50}$ = 1.7 μM) over GLP (IC$_{50}$ = 38 μM),[22] a second study using linear assay conditions for both enzymes revealed that **3a** inhibited GLP (IC$_{50}$ = 0.7 μM) as well as or better than G9a (IC$_{50}$ = 1.9 μM).[29] This observed selectivity difference is likely due to that the original study did not use identical assay conditions for both enzymes: the GLP assay was conducted under conditions where the reaction was oversaturated while the G9a assay was carried out under linear assay conditions. More recently, **3a** has been shown to be about 10-fold selective for GLP (IC$_{50}$ = 27 nM) over G9a (IC$_{50}$ = 250 nM) in chemi-luminescence-based oxygen tunneling (CLOT) assays.[30] Because no SAR was reported for this quinazoline scaffold, we decided to investigate multiple regions of this template to elucidate SAR and improve potency and selectivity. In our previous letter,[31] we reported preliminary SAR findings, the discovery of **10** (UNC0224) as a potent and selective G9a inhibitor, and a 1.7 Å X-ray crystal structure of the G9a−**10** complex, the first cocrystal structure of G9a with a small molecule inhibitor. In this article, we describe full accounts of the design, synthesis, biological evaluation, and SAR of compounds that explore three regions (i.e., 2-amino, 4-amino, and 7-methoxy) of this quinazoline scaffold. In particular,
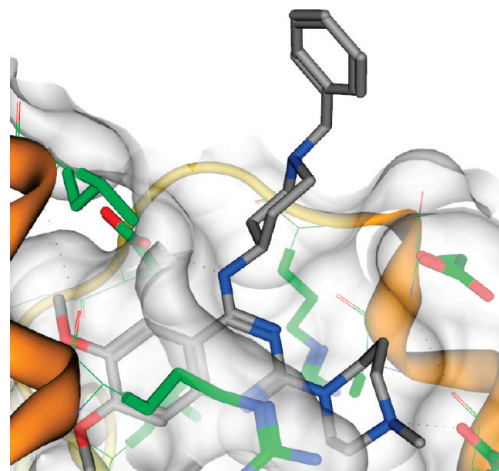
Figure 2. The lipophilic benzyl group (top) is exposed to solvent and does not makes any interactions with the protein in the X-ray crystal structure of the GLP−**3a** complex (PDB code: 3FPD).[29]
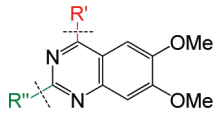
using the structural insights revealed by the G9a−**10** cocrystal structure, we optimized the 7-dimethylaminopropoxy side chain, which was not extensively explored in our previous letter.[31] This optimization resulted in the discovery of **29** (UNC0321) (Morrison K_i = 63 pM), the most potent G9a inhibitor to date.
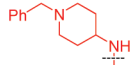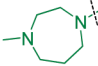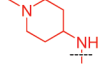
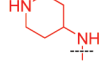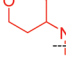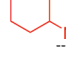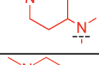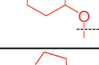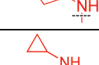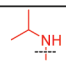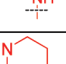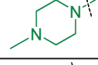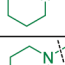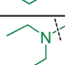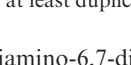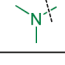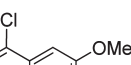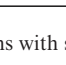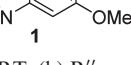## Results and Discussion

Our initial inhibitor design was based on the structural insights revealed by the X-ray crystal structure of the GLP−**3a** complex.[29] Because the benzyl group of **3a** is outside the peptide binding groove and does not make any interactions (Figure 2),[29] it was proposed that the 1-benzyl piperidin-4-yl-amino group (marked in red in Figure 1) of **3a** could be replaced with a smaller group such as 1-methyl piperidin-4-yl-amino and other smaller amino groups as shown in Table 1. This modification would lower the molecular weight, which is an important consideration for cellular activity. Additionally, exploration of the 2-amino region (marked in green in Figure 1) with various cyclic and acyclic amines shown in Table 1 was carried out.

An efficient two-step synthetic sequence was developed to prepare the compounds in Table 1 (Scheme 1). Displacing the 4-chloro of commercially available 2,4-dichloro-6,7-dimethoxyquinazoline (**1**) with the first set of amines at room temperature afforded the intermediates **2**. The displacement of the 2-chloro of the intermediates **2** with the second set of amines under microwave heating conditions yielded the desired 2,4-diamino-6,7-dimethoxyquinazolines **3**. Using this efficient synthesis, the compounds listed in Table 1 were rapidly prepared in high yields.

Newly synthesized compounds were evaluated in two orthogonal and complementary G9a biochemical assays: enzyme-coupled SAH detection (ECSD) and chemilumin-escence-based oxygen tunneling (CLOT). The ECSD assay monitors the conversion of cofactor SAM to SAH. This assay technology was previously employed to study *Schizosaccharomyces pombe* CLR4, a H3K9 specific PKMT.[32] The CLOT assay detects monomethylation of histone H3 peptide 1−11.[30] The use of these two orthogonal and complementary biochemical assays in parallel enables us to rule out false positives and other artifacts of one particular assay format and increases our confidence in SAR findings.

Table 1. SAR of 4- and 2-Amino Regions of the Quinazoline Template[a]

Compound ID	R'	R''	G9a IC$_{50}$ (nM)	
			ECSD	CLOT
3a	Ph-piperidine		180	250
3b	N-methyl piperidine		330	230
3c	HN-piperidine		< 30% inhibition at 1 µM	> 10,000
3d	tetrahydropyran		< 30% inhibition at 1 µM	> 10,000
3e	cyclohexyl		< 30% inhibition at 1 µM	> 10,000
3f			< 30% inhibition at 1 µM	> 10,000
3g			< 30% inhibition at 1 µM	> 10,000
3h	pyrrolidine		910	1,900
3i	cyclopropyl		< 30% inhibition at 1 µM	5,100
3j	isopropyl		< 30% inhibition at 1 µM	5,800
3k			< 30% inhibition at 1 µM	> 10,000
3l	N-methyl piperidine		150	200
3m		piperidine	550	510
3n		morpholine	1,600	810
3o			910	6,500
3p			1,100	900
2a		Cl	< 30% inhibition at 1 µM	9,100

[a] IC$_{50}$ values are the average of at least duplicate assay runs with standard deviation (SD) values that are 3-fold less than the average.

Scheme 1. Synthesis of 2,4-Diamino-6,7-dimethoxy Quinazolines **3**[a]
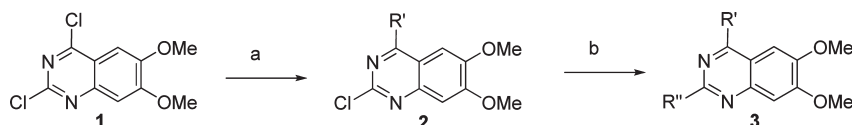
[a] (a) R' amines, DMF, DIEA, RT; (b) R'' amines, *i*-PrOH, 4 M HCl/dioxane, microwave, 160 °C.

For the 4-amino moiety of the quinazoline scaffold, replacing the *N*-(1-benzyl piperidin-4-yl)-amino group (**3a**) with the *N*-(1-methyl piperidin-4-yl)-amino group (**3b**) resulted in little or no potency loss (Table 1). This result confirmed our prediction that the benzyl group of **3a** could be replaced by a small alkyl group such as methyl in **3b** based on structural insights revealed by the cocrystal structure of the GLP−**3a** complex.[29] This SAR finding allowed us to reduce

the molecular weight while maintaining potency for this chemical series. On the other hand, replacing the *N*-(1-methyl piperidin-4-yl)-amino group (**3b**) with the *N*-(piperidin-4-yl)-amino (**3c**), *N*-(tetrahydropyran-4-yl)-amino (**3d**), or *N*-cyclohexyl-amino (**3e**) group led to significant potency loss, indicating that an alkylated nitrogen is important for inhibitory activity. We next explored the preferred substitution pattern (*N*,*N*-disubstitution versus *N*-monosubstitution) of the 4-amino group and whether the nitrogen could be replaced by an oxygen atom. Compound **3f** that contains a *N*-(1-methyl piperidin-4-yl),*N*-methyl-4-amino group was drastically less potent compared with compound **3b** that has a *N*-monosubstituted-4-amino group. Similarly, compound **3g**, an oxygen analogue of compound **3b**, had no G9a inhibitory activity in both assays. These results together indicate that the secondary nitrogen is important for G9a inhibition, likely via a hydrogen bond interaction. This finding was subsequently confirmed by the cocrystal structure of G9a-**10** (vide infra). Replacing the piperidine ring in **3b** with a smaller pyrrolidine ring (**3h**) led to some potency loss, but compound **3h**[33] still had appreciable G9a inhibitory activity. In addition, analogues containing a smaller amino group such as *N*-cyclopropyl-4-amino (**3i**), *N*-isopropyl-4-amino (**3j**), and *N*-methyl-4-amino (**3k**) were significantly less potent compared with compounds **3a** and **3b**.
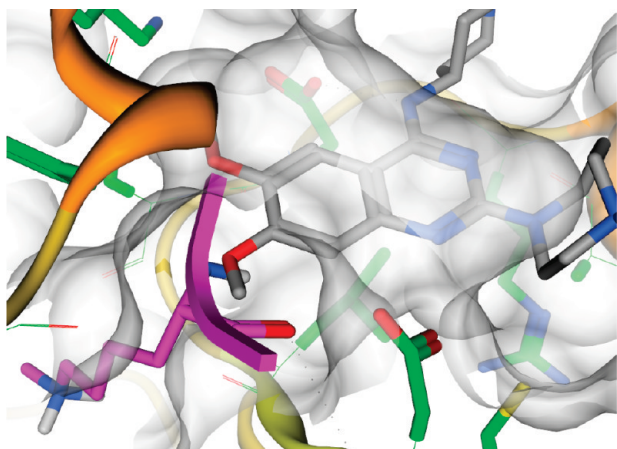
Figure 3. Compound **3a** (gray, red, and blue) does not occupy the lysine binding channel in the X-ray cocrystal structure of the GLP−**3a** complex (PDB code: 3FPD).[29] A fragment of the histone peptide (magenta) was transposed into this crystal structure to illustrate the lysine binding channel.

Modifications to the 2-amino region of the quinazoline template were well tolerated in general (Table 1). For example, the methyl homopiperazine group (**3b**) could be replaced with the methyl piperazine (**3l**) or piperidine (**3m**) group without significant potency loss. Analogues containing a morpholine (**3n**), diethylamine (**3o**), or dimethylamine (**3p**) group had moderate potency. The 2-choloro analogue **2a** had poor potency in both assays. In general, SAR trends from the ECSD and CLOT assays are in good agreement.

Having established tractable SAR for the 2- and 4-amino regions, we next explored the 7-methoxy moiety of the quinazoline scaffold, again using structure-based design and synthesis. The X-ray cocrystal structure of the GLP−**3a** complex revealed that **3a** occupied the GLP histone peptide binding site but did not interact with the narrow lysine binding channel (Figure 3).[29] To take advantage of this nearby lysine binding channel, it was hypothesized that adding a 7-aminoalkoxy side chain to the quinazoline template would make new interactions with the lysine binding channel while the rest of molecule maintained interactions with the peptide binding groove. Thus, compound **10** (structure shown in Scheme 2), which possesses a 7-dimethylaminopropoxy chain and also combines the best 2- and 4-amino moieties identified previously, was designed and modeled. Replacing GLP and **3a** in the X-ray cocrystal structure of the GLP−**3a** complex[29] with G9a and **10** yielded a model that suggests that **10** is capable of interacting with the narrow lysine binding channel. This docking model (not shown here) is virtually identical to the G9a-**10** X-ray cocrystal structure subsequently determined (vide infra).

To test this hypothesis, compound **10** was synthesized via the 10-step synthetic sequence outlined in Scheme 2. Benzyl protection of commercially available 2-methoxy-4-cyanophenol (**4**), followed by nitration and subsequent reduction of the nitro group afforded the aniline **5**, which was then converted to the quinazolinedione **6** via formation of methyl carbamate and subsequent saponification of the cyano group and ring closure. POCl$_3$ treatment of the quinazolinedione **6** afforded the 2,4-dichloro quinazoline **7**, which underwent two consecutive chloro displacement reactions to yield the 2,4-diamino quinazoline **8**. Debenzylation of the intermediate **8**, followed by a Mitsunobu reaction with 3-(dimethylamino)propan-1-ol, produced the desired compound **10**.

In G9a ECSD and CLOT assays, **10** was about 5-fold more potent compared to **3a** (Table 2). The high potency of **10** was confirmed in several secondary assays. In ITC experiments

Scheme 2. Synthesis of Compound **10**[a]
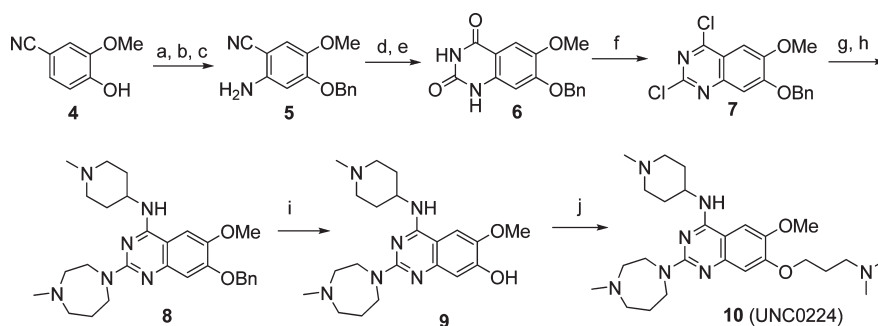
[a] (a) BnBr, K$_2$CO$_3$, DMF, RT; (b) HNO$_3$, Ac$_2$O, 0 °C to RT; (c) Fe dust, NH$_4$Cl, *i*-PrOH-H$_2$O, reflux, 67% over 3 steps; (d) methyl chloroformate, DIEA, DMF-DCM, 0 °C to RT; (e) NaOH, H$_2$O$_2$, EtOH, reflux, 70% over 2 steps; (f) *N*,*N*-diethylaniline, POCl$_3$, reflux, 59%; (g) 4-amino-1-methylpiperidine, DIEA, THF, RT; (h) 1-methylhomopiperazine, HCl, *i*-PrOH, 160 °C, microwave, 82% over 2 steps; (i) Pd/C, 1,4-cyclohexadiene, EtOH, reflux; (j) 3-(dimethylamino)propan-1-ol, PPh$_3$, DIAD, THF, 0 °C to RT, 46% over 2 steps.

that measure the binding affinity of a small molecule to the G9a protein,[34] **10** had about 5-fold higher binding affinity compared to **3a** (Table 2). In addition, **10** displaced a fluorescein labeled 15-mer H3 peptide (1−15) with higher efficiency than **3a** in a G9a fluorescence polarization (FP) assay and stabilized G9a better compared to **3a** in differential scanning fluorimetry (DSF) experiments.[31] These results together suggest that **10** is a more potent G9a inhibitor compared to **3a**.

A high resolution (1.7 Å) X-ray cocrystal structure of the G9a−**10** complex was obtained. This cocrystal structure, the first X-ray crystal structure of G9a in complex with a small molecule inhibitor, revealed that the 7-dimethylamino propoxy side chain of **10** indeed occupied the lysine binding channel of G9a and the basic nitrogen interacted with Tyr1154 and Leu1086 (Figure 4), thus validating our binding hypothesis. The higher potency of **10** compared to **3a** can be explained by these additional interactions between the 7-dimethylamino propoxy side chain and the lysine binding channel. These interactions were absent in the GLP−**3a** complex as shown in Figure 3. Other key structural insights revealed by the G9a−**10** cocrystal structure include: (1) the bulk of **10** occupied the histone peptide binding site, similar to the GLP−**3a** complex, (2) the hydrogen of the secondary amino group at the 4-position formed a hydrogen bond with Asp1083, providing a potential explanation for the drastic potency loss of compound **3f** compared to compound **3b** (Table 1), and (3) the lysine binding channel was not fully occupied by the 7-dimethylamino propoxy group and there is space at the end of the channel to accommodate a longer chain or larger amino group (Figure 5).

On the basis of this observation, the compounds in Tables 3−5 were designed and synthesized to extensively explore the SAR of this 7-aminoalkoxy region and optimize

potency of this series. Compounds **11**, **14−16**, **19−23**, **25−29** were synthesized from the phenol **9** via Mitsunobu reactions with corresponding alcohols (Scheme 3), similar to the synthesis of **10**. Compound **24** was made via Mitsunobu reaction of the phenol **9** with the Boc-protected 5-amino-1-pentanol, followed by the deprotection of the Boc group. Compounds **12**, **13**, **17**, and **18** were synthesized from the chlorides **30**, which were prepared from the phenol **9** via Mitsunobu reactions with corresponding chloroalkyl alcohols.

These newly synthesized compounds bearing various 7-alkoxy side chains were evaluated in G9a ECSD and CLOT assays and SAR results are summarized in Tables 3−5. Compounds **11**, **10**, **12**, and **13** that contain, respectively, a 2−5-carbon chain, had similar potency while the 6-carbon chain containing analogue **14** was significantly less potent (Table 3), indicating the lysine binding channel of G9a can accommodate a longer aminoalkoxy side chain up to 5 carbons in length. Compounds possessing various amino capping groups were evaluated next (Table 4). Compounds **15**, **16**, and **17** containing, respectively, *N*-methylamino, *N,N*-diethylamino, and *N*-methyl,*N*-propylamino groups, were as potent as **10**, which has
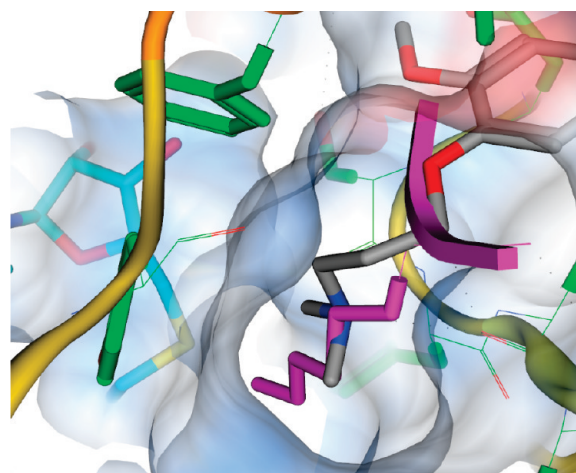
Figure 5. The 7-dimethylamino propoxy side chain (gray, blue, and red) of **10** does not fully occupy the lysine binding channel in the X-ray crystal structure of the G9a−**10** complex (PDB code: 3K5K). A fragment of the H3K9 peptide (magenta) was transposed into this crystal structure to illustrate the lysine binding channel.
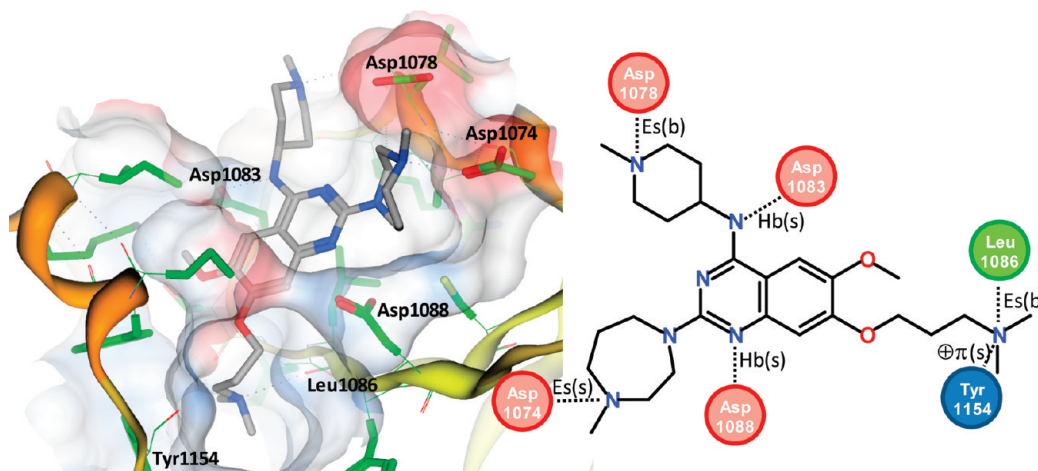
Table 2. Potency Comparison of **10** with **3a**[a]

| | G9a | | |
compd	ECSD IC$_{50}$ (nM)	CLOT IC$_{50}$ (nM)	ITC K_d (nM)
10	43	57	23
3a	180	250	130

[a] IC$_{50}$ and K_d values are the average of at least duplicate assay runs with SD values that are 3-fold less than the average.
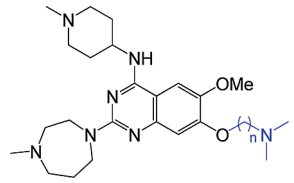

Figure 4. X-ray crystal structure of the G9a−**10** complex (PDB code: 3K5K). The inhibitor−protein interactions are annotated as follows: "Es", electrostatic; "Hb", hydrogen bonding; "⊕π", cation−π interactions; "(s)", interaction with a side chain; "(b)", interaction with the backbone.

Table 3. SAR of the Chain Length[a]

compd	n	G9a IC$_{50}$ (nM)	
		ECSD	CLOT
11	2	110	120
10	3	43	57
12	4	140	110
13	5	95	49
14	6	1500	3200

[a] IC$_{50}$ values are the average of at least duplicate assay runs with SD values that are 3-fold less than the average.
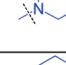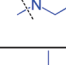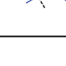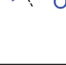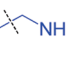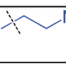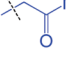
a *N,N*-dimethylamino group. Similarly, replacing the tertiary amino group of compound **13** with the primary amino group (compound **24**) did not result in significant potency loss. Cyclic amino groups were also explored. Although the morpholine **20** was >10-fold less potent, the pyrrolidine **18** and piperidine **19** were more potent compared to their acyclic amine analogues such as **16**. In particular, the pyrrolidine **18** with a respective IC$_{50}$ of 8 and 11 nM in ECSD and CLOT assays was about 5-fold more potent than **10**. These results together suggest that modifications to the substituents on the basic nitrogen are well tolerated and a larger amino capping group can be accommodated. These SAR findings are consistent with the structural insights revealed by the cocrystal structure of the G9a−**10** complex (vide supra).

The necessity for a basic nitrogen in the aminoalkoxy side chain was investigated next (Table 4). Replacing the nitrogen in the 7-dimethylamino propoxy group of **10** with a methine (**21**) led to about a 100-fold potency loss. Switching the *N,N*-dimethylamino group in compound **12** to the methoxy group in compound **22** or the *N*-Boc protected amino group in compound **23** completely abolished G9a inhibitory activity. Similarly, compound **25** that contains an amide group was about 100-fold less potent compared to its amine analogue **24**. Taken together, these results suggest that the basic nitrogen in the aminoalkoxy side chain is critical for retaining high potency for G9a.

In addition, it was found that replacing the 5-carbon chain in compound **13** with an ethoxyethyl chain resulted in compound **29** (IC$_{50}$ = 6 nM (CLOT) and 9 nM (ECSD)), the most potent G9a inhibitor to date (Table 5). Increasing the size of the amino capping group from dimethylamino (**29**) to pyrrolidine (**26**) led to > 5-fold potency decrease. Compound **27** that possesses a 2-(*N*-ethyl,*N*-methylamino) ethyl chain was also less potent compared to its carbon analogue **13** and oxygen analogue **29**. Additionally, conformationally constrained analogues were explored. For example, compound **28**[33] containing a (piperidin-3-yl)methoxy group was significantly less potent compared to its acyclic analogues **15** and **17**. In general, the extensive exploration of the 7-aminoalkoxy region of this quinazoline scaffold yielded valuable SAR findings, which are useful for future inhibitor design.

Because compound **29** likely reached the IC$_{50}$ limits of the G9a ECSD and CLOT assays, a newly developed endoproteinase-coupled microfluidic capillary electrophoresis (MCE) assay[35] that is suitable for mechanism of action and kinetics
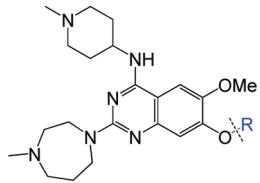
Table 4. SAR of the Capping Group[a]

Compound ID	R	G9a IC$_{50}$ (nM)	
		ECSD	CLOT
15		120	45
16		52	65
17		51	45
18		8.0	11
19		25	20
20		880	780
21		3,400	5,200
22		< 30% inhibition at 1 μM	> 10,000
23		< 30% inhibition at 1 μM	> 10,000
24		235	110
25		< 30% inhibition at 1 μM	> 10,000

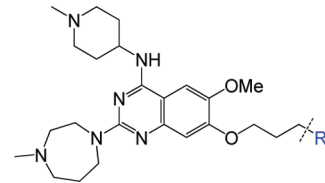[a] IC$_{50}$ values are the average of at least duplicate assay runs with SD values that are 3-fold less than the average.
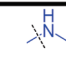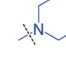
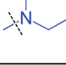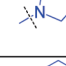studies of G9a inhibitors was utilized to determine the Morrison K_i, which is an effective method developed by Morrison and co-workers that uses a quadratic fit for steep dose response data over a narrow compound concentration range for assessing tight binding inhibitors.[36,37] As shown in Figure 6, **29** had a Morrison K_i of 63 pM and was about 40-fold more potent than **10** (Morrison K_i = 2.6 nM) and 250-fold more potent than **3a** (Morrison K_i = 16 nM) in this G9a MCE assay. In addition, the Morrison K_i (2.6 nM) of **10** matched well with its K_i (1.6 nM),[35] which was previously determined using this G9a MCE assay.

The selectivity of compounds **29**, **10**, and **3a** were evaluated next. As shown in Table 6, **3a** was more selective for GLP over G9a in ECSD assays. This result is consistent with the previous finding: **3a** was about 10-fold selective for GLP over G9a in CLOT assays.[30] In contrast to **3a**, **29** inhibited G9a as

Table 5. Additional SAR of the 7-Aminoalkoxy Side Chain[a]

Compound ID	R	G9a IC$_{50}$ (nM)	
		ECSD	CLOT
29		9.0	6.0
26		57	110
27		345	173
28		1,500	5,100

[a] IC$_{50}$ values are the average of at least duplicate assay runs with SD values that are 3-fold less than the average.

Scheme 3. Synthesis of Compounds **11−29**[a]
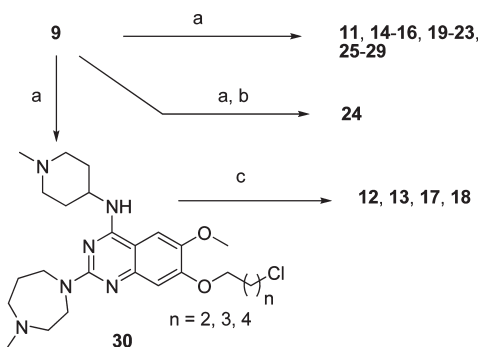
[a] (a) various alcohols, PPh$_3$, DIAD, THF, 0 °C to RT; (b) TFA, DCM, RT; (c) various amines, *i*-PrOH, 160 °C, microwave.

well as or better than GLP while **10** was equipotent versus G9a and GLP in both ECSD and CLOT assays. This different selectivity profile makes **29** and **10** potentially useful tool compounds that are complementary to **3a**. In addition to G9a and GLP, compounds **29** and **10** were evaluated in SET7/9 (a H3K4 PKMT), SET8/PreSET7 (a H4K20 PKMT), and PRMT3 (a protein arginine methyltransferase (PRMT)) ECSD assays and found to be inactive (IC$_{50}$ > 40 μM) versus these protein lysine and arginine methyltransferases, providing a >1000-fold selectivity window for G9a over these PKMTs and PRMT. **29** and **10** were also inactive (IC$_{50}$ > 57 μM) in the

Figure 6. Morrison K_is of compounds **29**, **10**, and **3a** in the G9a MCE assay.

formaldehyde dehydrogenase-coupled biochemical assay of JMJD2E,[38] a Jumonji protein demethylase. Additionally, **10** was clean (less than 20% inhibition at 1 μM) against a broad range of G-protein coupled receptors, ion channels, and transporters in a 30-target selectivity panel (tested by MDS Pharma Services) with the exception of 82% inhibition of the muscarinic M$_2$ receptor at 1 μM and 31% inhibition of the histamine H$_1$ receptor at 1 μM.

Conclusions

Inhibitor design and synthesis based on the GLP−**3a** X-ray cocrystal structure in combination with early SAR exploration led to the discovery of **10**, a 2,4-diamino-7-aminoalkoxy-quinazoline, as a potent and selective inhibitor of PKMT G9a. A high resolution X-ray crystal structure of the G9a−**10** complex, the first cocrystal structure of G9a with a small molecule inhibitor, was obtained. This high resolution cocrystal structure of the G9a−**10** complex validated our binding and inhibitor design hypothesis. Using the structural insights revealed by this cocrystal structure, the 7-dimethylaminopropoxy side chain of **10** was optimized, resulting in the discovery of **29** (Morrison K_i = 63 pM), the most potent G9a inhibitor to date. Exploration of the 2-amino, 4-amino, and 7-aminoalkoxy regions of this quinazoline scaffold yielded valuable SAR findings, which can be exploited for design of novel inhibitors in the future. Compounds **29** and **10** are potentially useful small molecule tools for the biomedical research community to investigate the biology of G9a and its role in chromatin remodeling as well as PTMs of other proteins.

Experimental Section

Chemistry General Procedures. HPLC spectra of all compounds except **3k**, **10−14**, **17−20**, **22**, **23**, **25**, and **27−29** were acquired from an Agilent 6110 series system with UV detector set to 254 nm. Samples were injected (5 μL) onto an Agilent Eclipse Plus 4.6 mm × 50 mm, 1.8 μM, C18 column at room temperature. A linear gradient from 10% to 100% B (MeOH + 0.1% acetic acid) in 5.0 min was followed by pumping 100% B for another 2 min with A being H$_2$O + 0.1% acetic acid. The flow rate was 1.0 mL/min. The HPLC spectra of **3k**, **10−14**, **17−20**, **22**, **23**, **25**, and **27−29** were recorded from an Agilent

Table 6. Selectivity of Compounds **29**, **10**, and **3a**[a]

compd	G9a IC$_{50}$ (nM)		GLP IC$_{50}$ (nM)		SET7/9 IC$_{50}$ (nM)	SET8/PreSET7 IC$_{50}$ (nM)	PRMT3 IC$_{50}$ (nM)	JMJD2E IC$_{50}$ (nM)
	ECSD	CLOT	ECSD	CLOT				
29	9.0	6.0	15	23	>40000	>40000	>40000	>57000
10	43	57	50	58	>40000	>40000	>40000	>57000
3a	180	250	34	27	ND	ND	ND	ND

[a] IC$_{50}$ values are the average of at least duplicate assay runs with SD values that are 3-fold less than the average. ND: not determined.

6110 series system with UV detector set to 254 nm. Samples were injected (10 μL) onto a Phenomenex Kinetex 2.6 μM, 100 mm × 2.1 mm, C18 column at room temperature. Then they were eluted out with 72% B (MeCN) and A being H_2O + 0.1% formic acid. The flow rate was 0.3 mL/min. Mass spectra (MS) data were acquired in positive ion mode using an Agilent 6110 single quadrupole mass spectrometer with an electrospray ionization (ESI) source. High-resolution (negative ion) mass spectra (HRMS) were acquired using a Shimadzu LCMS-IT-Tof time-of-flight mass spectrometer. Nuclear magnetic resonance (NMR) spectra were recorded at Varian Mercury spectrometer with 400 MHz for proton (^{1}H NMR) and 100 MHz for carbon (^{13}C NMR) or Varian 300 MHz for proton (^{1}H NMR); chemical shifts are reported in ppm (δ). Preparative HPLC was performed on Agilent Prep 1200 series with UV detector set to 220 nm. Samples were injected onto a Phenomenex Luna 75 mm × 30 mm, 5 μM, C18 column at room temperature. The flow rate was 30 mL/min. Various linear gradients were used with A being H_2O + 0.5% TFA and B being MeOH. HPLC was used to establish the purity of targeted compounds. All compounds that were evaluated in biological assays had >95% purity using the HPLC methods described above.

N-(1-Benzylpiperidin-4-yl)-6,7-dimethoxy-2-(4-methyl-1,4-diazepan-1-yl)quinazolin-4-amine (3a). 4-Amino-1-benzylpiperidine (6.8 mL, 36.02 mmol) was added to a solution of 2,4-dichloro-6,7-dimethoxyquinazoline (**1**, 4.22 g, 16.28 mmol) in DMF (40 mL), followed by the addition of *N,N*-diisopropylethylamine (3 mL, 17.24 mmol), and the resulting mixture was stirred at room temperature for 2 h until TLC showed that the starting material had disappeared. Water was added to the reaction mixture, and the resulting solution was extracted with ethyl acetate. The organic layer was washed with 0.5% acetic acid aqueous solution and brine, dried, and concentrated to give the crude product, which was purified on an ISCO chromatography system using 40 g silica gel column eluting with hexane–ethyl acetate to give 6.2 g of the desired compound as a yellow solid, yield 92%. ^{1}H NMR (300 MHz, MeOH-d_4) δ ppm 7.70 (s, 1H), 7.59–7.42 (m, 5H), 7.11 (s, 1H), 4.47–4.36 (m, 1H), 4.09 (s, 3H), 4.08 (s, 3H), 3.87 (s, 2H), 3.26 (d, J = 12.0 Hz, 2H), 2.61–2.52 (m, 2H), 2.24 (d, J = 12.0 Hz, 2H), 2.02–1.82 (m, 2H). HPLC: 99%, RT 4.112 min. MS (ESI) 413 [M + H]$^+$. *N*-(1-Benzylpiperidin-4-yl)-2-chloro-6,7-dimethoxyquinazolin-4-amine (232 mg, 0.56 mmol) was dissolved in 3 mL of isopropyl alcohol. To this solution was added 1-methylhomopiperazine (0.14 mL, 1.12 mmol) and HCl in dioxane (4.0 M, 0.28 mL, 1.12 mmol). The resulting solution was heated using microwave irradiation to 160 °C for 10 min. After cooling, TLC indicated the completion of the reaction. After removal of the solvent by rotary evaporation, the residue was redissolved in CH_2Cl_2 and washed with saturated $NaHCO_3$ solution. The organic layer was dried, concentrated, and purified by ISCO to give 221.2 mg of the desired compound **3a** as a yellow solid, yield 80%. ^{1}H NMR (400 MHz, MeOH-d_4) δ ppm 7.36 (s, 1H), 7.32–7.24 (m, 5H), 6.87 (s, 1H), 4.09 (m, 1H), 3.89 (m, 2H), 3.86 (s, 3H), 3.85 (s, 3H), 3.81 (t, J = 4 Hz, 2H), 3.53 (s, 2H), 2.96 (d, J = 12 Hz, 2H), 2.71 (m, 2H), 2.56 (m, 2H), 2.32 (s, 3H), 2.14 (t, J = 12 Hz, 2H), 2.06 (d, J = 12 Hz, 2H), 1.98 (m, 2H), 1.69 (m, 2H). HPLC: 100%, RT 2.044 min. MS (ESI) 491 [M + H]$^+$.

6,7-Dimethoxy-2-(4-methyl-1,4-diazepan-1-yl)-*N*-(1-methyl-piperidin-4-yl)quinazolin-4-amine (3b). 4-Amino-1-methylpiperidine (1.12 mL, 8.92 mmol) was added to a solution of 2,4-dichloro-6,7-dimethoxyquinazoline (**1**, 1.05 g, 4.05 mmol) in THF (10 mL), followed by the addition of *N,N*-diisopropylethylamine (1.41 mL, 8.11 mmol), and the resulting mixture was stirred at room temperature for 2 h until the TLC indicated that the reaction completed. The solvent was removed on the rotary evaporation, and the residue was purified by an ISCO chromatography system using 40 g silica gel column eluting with hexane–ethyl acetate to give 1.26 g of the targeted compound **2a** as a yellow solid, yield 92%. ^{1}H NMR (300 MHz, DMSO-d_6) δ ppm 8.13 (d, J = 7.4 Hz, 1H), 7.78 (s, 1H), 7.18 (s, 1H), 4.28–4.10

(m, 1H), 4.00 (s, 3H), 4.02 (s, 3H), 2.96 (d, J = 11.5 Hz, 2H), 2.32 (s, 3H), 2.19–1.95 (m, 4H), 1.84–1.71 (m, 2H). HPLC: 100%, RT 4.148 min. MS (ESI) 333 [M + H]$^+$. **3b** (239.5 mg, yield 78%) was prepared as a yellow solid from 2-chloro-6,7-dimethoxy-*N*-(1-methylpiperidin-4-yl)quinazolin-4-amine (**2a**, 247.6 mg, 0.74 mmol), 1-methylhomopiperazine (0.18 mL, 1.47 mmol), HCl in dioxane (4.0 M, 0.37 mL, 1.47 mmol), and isopropyl alcohol (3 mL) using the same procedure as **3a**. ^{1}H NMR (400 MHz, MeOH-d_4) δ ppm 7.38 (s, 1H), 6.89 (s, 1H), 4.15–4.07 (m, 1H), 3.93–3.89 (m, 2H), 3.88 (s, 3H), 3.87 (s, 3H), 3.82 (t, J = 6.4 Hz, 2H), 2.94 (d, J = 12.1 Hz, 2H), 2.76–2.70 (m, 2H), 2.60–2.57 (m, 2H), 2.34 (s, 3H), 2.30 (s, 3H), 2.17 (td, J = 12.1, 2.2 Hz, 2H), 2.12–2.04 (m, 2H), 2.04–1.96 (m, 2H), 1.76–1.66 (m, 2H). ^{13}C NMR (100 MHz, MeOH-d_4) δ ppm 160.24, 159.36, 156.07, 147.11, 105.26, 104.84, 104.28, 59.62, 58.19, 56.98, 56.39, 56.12, 46.97, 46.71, 46.63, 46.31, 32.38, 28.43. HPLC: 100%, RT 0.571 min. MS (ESI) 415 [M + H]$^+$. HRMS calcd for $C_{22}H_{34}N_6O_2$: 414.2743. Found: 413.2685 [M − H].

6,7-Dimethoxy-2-(4-methyl-1,4-diazepan-1-yl)-*N*-(piperidin-4-yl)quinazolin-4-amine (3c). 3c was prepared as a yellow solid by the same procedure as **3b**, yield 81%. ^{1}H NMR (400 MHz, MeOH-d_4) δ ppm 7.05 (s, 1H), 6.97 (s, 1H), 4.15 (d, J = 13.3 Hz, 2H), 4.00–3.95 (m, 2H), 3.94 (s, 3H), 3.91–3.85 (m, 5H), 3.12–3.06 (m, 2H), 3.01–2.92 (m, 1H), 2.80–2.73 (m, 2H), 2.64–2.57 (m, 2H), 2.38 (s, 3H), 2.10–1.94 (m, 4H), 1.67–1.57 (m, 2H). ^{13}C NMR (100 MHz, MeOH-d_4) δ ppm 166.40, 159.50, 156.35, 152.68, 146.43, 106.55, 106.24, 106.22, 59.70, 58.28, 56.71, 56.41, 50.25, 50.03, 47.02, 46.81, 46.68, 35.56, 28.49. HPLC: 100%, RT 0.670 min. MS (ESI) 401 [M + H]$^+$.

6,7-Dimethoxy-2-(4-methyl-1,4-diazepan-1-yl)-*N*-(tetrahydro-2*H*-pyran-4-yl)quinazolin-4-amine (3d). 3d was prepared as an off-white solid by the same procedure as **3b**, yield 84%. ^{1}H NMR (400 MHz, MeOH-d_4) δ ppm 7.44 (s, 1H), 6.95 (s, 1H), 4.44–4.36 (m, 1H), 4.08–4.05 (m, 2H), 4.00–3.95 (m, 2H), 3.94 (s, 3H), 3.93 (s, 3H), 3.89 (t, J = 6.3 Hz, 2H), 3.60 (t, J = 11.9 Hz, 2H), 2.83–2.77 (m, 2H), 2.69–2.63 (m, 2H), 2.41 (s, 3H), 2.10–2.04 (m, 4H), 1.83–1.72 (m, 2H). ^{13}C NMR (100 MHz, MeOH-d_4) δ ppm 160.15, 160.12, 155.92, 150.15, 146.84, 105.89, 104.89, 104.17, 68.53, 59.83, 58.27, 56.96, 56.32, 46.91, 46.78, 46.70, 34.04, 28.60. HPLC: 100%, RT 1.316 min. MS (ESI) 402 [M + H]$^+$.

***N*-Cyclohexyl-6,7-dimethoxy-2-(4-methyl-1,4-diazepan-1-yl)-quinazolin-4-amine (3e). 3e** was prepared as a yellow solid by the same procedure as **3b**, yield 82%. ^{1}H NMR (400 MHz, MeOH-d_4) δ ppm 7.38 (s, 1H), 6.89 (s, 1H), 4.12–4.04 (m, 1H), 3.93–3.89 (m, 2H), 3.88 (s, 3H), 3.87 (s, 3H), 3.82 (t, J = 6.4 Hz, 2H), 2.76–2.70 (m, 2H), 2.60–2.54 (m, 2H), 2.33 (s, 3H), 2.10–2.04 (m, 2H), 2.03–1.95 (m, 2H), 1.85–1.81 (m, 2H), 1.75–1.66 (m, 1H), 1.44–1.34 (m, 4H), 1.28–1.21 (m, 1H). ^{13}C NMR (100 MHz, MeOH-d_4) δ ppm 159.97, 159.92, 155.76, 149.54, 146.76, 105.64, 104.94, 104.27, 59.75, 58.16, 56.96, 56.29, 51.77, 46.90, 46.74, 46.71, 33.93, 28.53, 27.17, 26.92. HPLC: 100%, RT 2.841 min. MS (ESI) 400 [M + H]$^+$.

6,7-Dimethoxy-*N*-methyl-2-(4-methyl-1,4-diazepan-1-yl)-*N*-(1-methylpiperidin-4-yl)quinazolin-4-amine (3f). 3f was prepared as an off-white solid by the same procedure as **3b**, yield 80%. ^{1}H NMR (400 MHz, MeOH-d_4) δ ppm 7.14 (s, 1H), 6.96 (s, 1H), 4.29–4.19 (m, 1H), 3.94 (m, 5H), 3.90–3.83 (m, 5H), 3.15 (s, 3H), 3.02 (d, J = 11.5 Hz, 2H), 2.79–2.71 (m, 2H), 2.64–2.56 (m, 2H), 2.37 (s, 3H), 2.32 (s, 3H), 2.15 (t, J = 11.5 Hz, 2H), 2.10–1.97 (m, 4H), 1.92 (d, J = 10.5 Hz, 2H). ^{13}C NMR (100 MHz, MeOH-d_4) δ 165.57, 159.30, 155.99, 153.00, 145.83, 107.08, 106.21, 106.19, 59.79, 58.70, 58.26, 56.81, 56.55, 56.35, 46.94, 46.80, 46.74, 46.31, 34.55, 29.61, 28.59. HPLC: 100%, RT 0.868 min. MS (ESI) 429 [M + H]$^+$.

6,7-Dimethoxy-2-(4-methyl-1,4-diazepan-1-yl)-4-(1-methyl-piperidin-4-yloxy)quinazoline (3g). 3g was prepared as a yellow solid by the same procedure as **3b**, yield 77%. ^{1}H NMR (400 MHz, MeOH-d_4) δ 7.25 (s, 1H), 6.99 (s, 1H), 5.38–5.28 (m, 1H), 4.00–3.93 (m, 5H), 3.93–3.86 (m, 5H), 2.88–2.75 (m, 4H), 2.67–2.60 (m, 2H), 2.52–2.42 (m, 2H), 2.40 (s, 3H), 2.37 (s, 3H),

2.23−2.13 (m, 2H), 2.10−1.93 (m, 4H). HPLC: 99%, RT 1.724 min. MS (ESI) 416 [M + H]$^+$.

6,7-Dimethoxy-2-(4-methyl-1,4-diazepan-1-yl)-N-(1-methylpyrrolidin-3-yl)quinazolin-4-amine (3h). 3h was prepared as a yellow solid by the same procedure as **3b**, yield 79%. ^{1}H NMR (400 MHz, MeOH-d_4) δ 7.39 (s, 1H), 6.94 (s, 1H), 4.84−4.74 (m, 1H), 4.00−3.95 (m, 2H), 3.93 (s, 3H), 3.92 (s, 3H), 3.88 (t, $J = 6.3$ Hz, 2H), 3.00 (dd, $J = 9.8, 7.1$ Hz, 1H), 2.87−2.75 (m, 3H), 2.72−2.60 (m, 4H), 2.50−2.41 (m, 4H), 2.39 (s, 3H), 2.09−2.01 (m, 2H), 2.01−1.92 (m, 1H). ^{13}C NMR (100 MHz, MeOH-d_4) δ 160.43, 159.98, 156.01, 149.97, 146.91, 105.84, 104.83, 104.08, 63.66, 59.83, 58.26, 56.95, 56.34, 56.24, 52.25, 46.93, 46.78, 46.65, 42.48, 33.18, 28.57. HPLC: 100%, RT 0.528 min. MS (ESI) 401 [M + H]$^+$.

N-Cyclopropyl-6,7-dimethoxy-2-(4-methyl-1,4-diazepan-1-yl)-quinazolin-4-amine (3i). 3i was prepared as a yellow solid by the same procedure as **3b**, yield 79%. ^{1}H NMR (400 MHz, MeOH-d_4) δ ppm 7.17 (s, 1H), 6.80 (s, 1H), 5.38 (s, 0.34 H, NH), 3.91−3.84 (m, 2H), 3.83−3.71 (m, 8H), 2.85−2.79 (m, 1H), 2.68−2.64 (m, 2H), 2.52−2.48 (m, 2H), 2.25 (s, 3H), 1.97−1.89 (m, 2H), 0.73−0.67 (m, 2H), 0.55−0.50 (m, 2H). HPLC: 100%, RT 2.631 min. MS (ESI) 358 [M + H]$^+$.

N-Isopropyl-6,7-dimethoxy-2-(4-methyl-1,4-diazepan-1-yl)-quinazolin-4-amine (3j). 3j was prepared as a yellow solid by the same procedure as **3b**, yield 76%. ^{1}H NMR (400 MHz, MeOH-d_4) δ 7.38 (s, 1H), 6.90 (s, 1H), 5.48 (s, 1H, NH), 4.47 (dt, $J = 13.1, 6.6$ Hz, 1H), 3.97−3.91 (m, 2H), 3.89 (s, 3H), 3.88 (s, 3H), 3.84 (t, $J = 6.4$ Hz, 2H), 2.76−2.71 (m, 2H), 2.61−2.55 (m, 2H), 2.34 (s, 3H), 2.05−1.97 (m, 2H), 1.31 (d, $J = 6.6$ Hz, 6H). HPLC: 99%, RT 2.532 min. MS (ESI) 360 [M + H]$^+$.

6,7-Dimethoxy-N-methyl-2-(4-methyl-1,4-diazepan-1-yl)quinazolin-4-amine (3k). 3k was prepared as a yellow solid by the same procedure as **3b**, yield 78%. ^{1}H NMR (400 MHz, CDCl$_3$) δ 6.89 (s, 1H), 6.76 (s, 1H), 5.34 (s, 1H), 4.06−3.97 (m, 2H), 3.95−3.83 (m, 8H), 3.10 (d, $J = 4.7$ Hz, 3H), 2.73−2.67 (m, 2H), 2.60−2.52 (m, 2H), 2.36 (s, 3H), 2.08−1.95 (m, 2H). HPLC: 100%, RT 0.673 min. MS (ESI) 332 [M + H]$^+$.

6,7-Dimethoxy-2-(4-methylpiperazin-1-yl)-N-(1-methylpiperidin-4-yl)quinazolin-4-amine (3l). 3l was prepared as a yellow solid by the same procedure as **3b**, yield 78%. ^{1}H NMR (400 MHz, MeOH-d_4) δ ppm 7.39 (s, 1H), 6.85 (s, 1H), 4.16−4.08 (m, 1H), 3.88 (s, 3H), 3.87 (s, 3H), 3.80 (m, 4H), 2.94 (d, $J = 12.1$ Hz, 2H), 2.55−2.45 (m, 4H), 2.31 (s, 3H), 2.30 (s, 3H), 2.22−2.16 (m, 2H), 2.11−2.02 (m, 2H), 1.76−1.66 (m, 2H). HPLC: 100%, RT 1.068 min. MS (ESI) 401 [M + H]$^+$.

6,7-Dimethoxy-N-(1-methylpiperidin-4-yl)-2-(piperidin-1-yl)-quinazolin-4-amine (3m). 3m was prepared as a yellow solid by the same procedure as **3b**, yield 80%. ^{1}H NMR (400 MHz, MeOH-d_4) δ ppm 7.64 (s, 1H), 7.11 (s, 1H), 4.58−4.46 (m, 1H), 3.94 (s, 3H), 3.90 (s, 3H), 3.87−3.81 (m, 4H), 3.63 (d, $J = 12.8$ Hz, 2H), 3.26−3.19 (m, 1H), 2.89 (s, 3H), 2.34 (d, $J = 12.9$ Hz, 2H), 2.10−1.96 (m, 2H), 1.82−1.66 (m, 7H). HPLC: 100%, RT 3.896 min. MS (ESI) 386 [M + H]$^+$.

6,7-Dimethoxy-N-(1-methylpiperidin-4-yl)-2-morpholinoquinazolin-4-amine (3n). 3n was prepared as a yellow solid by the same procedure as **3b**, yield 81%. ^{1}H NMR (400 MHz, MeOH-d_4) δ ppm 7.40 (s, 1H), 6.86 (s, 1H), 4.17−4.09 (m, 1H), 3.88 (s, 3H), 3.87 (s, 3H), 3.73 (s, 8H), 2.94 (d, $J = 11.8$ Hz, 2H), 2.31 (s, 3H), 2.19 (t, $J = 12.2$ Hz, 2H), 2.10−2.04 (m, 2H), 1.77−1.67 (m, 2H). HPLC: 100%, RT 0.554 min. MS (ESI) 388 [M + H]$^+$.

N^2,N^2-diethyl-6,7-dimethoxy-N^4-(1-methylpiperidin-4-yl)quinazoline-2,4-diamine (3o). 3o was prepared as a yellow solid by the same procedure as **3b**, yield 77%. ^{1}H NMR (400 MHz, MeOH-d_4) δ ppm 7.39 (s, 1H), 6.92 (s, 1H), 4.20−4.13 (m, 1H), 3.91 (s, 3H), 3.90 (s, 3H), 3.66 (q, $J = 7.0$ Hz, 4H), 2.97 (d, $J = 12.0$ Hz, 2H), 2.33 (s, 3H), 2.20 (dd, $J = 12.1, 2.3$ Hz, 2H), 2.16−2.07 (m, 2H), 1.73 (qd, $J = 12.3, 3.7$ Hz, 2H), 1.22 (t, $J = 7.0$ Hz, 6H). ^{13}C NMR (100 MHz, MeOH-d_4) δ ppm 160.28, 159.73, 155.77, 150.28, 146.53, 105.74, 104.73, 104.23, 56.95, 56.27, 46.41, 42.93, 32.63, 14.24. HPLC: 100%, RT 2.711 min. MS (ESI) 374 [M + H]$^+$.

6,7-Dimethoxy-N^2,N^2-dimethyl-N^4-(1-methylpiperidin-4-yl)-quinazoline-2,4-diamine (3p). 3p was prepared as a white solid by the same procedure as **3b**, yield 76%. ^{1}H NMR (400 MHz, MeOH-d_4) δ ppm 7.44 (s, 1H), 6.94 (s, 1H), 4.25−4.17 (m, 1H), 3.94 (s, 3H), 3.92 (s, 3H), 3.21 (s, 6H), 3.00 (d, $J = 12.5$ Hz, 2H), 2.35 (s, 3H), 2.27−2.20 (m, 2H), 2.19−2.11 (m, 2H), 1.81−1.71 (m, 2H). ^{13}C NMR (100 MHz, MeOH-d_4) δ ppm 161.04, 160.21, 155.91, 149.84, 146.82, 105.65, 104.67, 104.28, 56.99, 56.32, 56.24, 46.41, 37.73, 32.46. HPLC: 99%, RT 2.623 min. MS (ESI) 346 [M + H]$^+$.

2-Amino-4-benzyloxy-5-methoxybenzonitrile (5). To an ice-cooled solution of 4-hydroxy-3-methoxybenzonitrile (3.40 g, 22.8 mmol) in DMF (45 mL) was slowly added potassium carbonate (4.73 g, 34.2 mmol) and then benzyl bromide (3.0 mL, 25.1 mmol). The reaction mixture was stirred overnight at room temperature, and saturated sodium chloride aqueous solution (80 mL) was added. The resulting precipitate was collected, washed with water and dried to provide 4-benzyloxy-3-methoxybenzonitrile as a yellow solid (5.40 g, 93% yield). ^{1}H NMR (400 MHz, CDCl$_3$) δ ppm 7.36−7.27 (m, 5H), 7.14 (dd, $J = 8.4, 2.0$ Hz, 1H), 7.02 (d, $J = 2.0$ Hz, 1H), 6.83 (d, $J = 8.4$ Hz, 1H), 5.13 (s, 2H), 3.83 (s, 3H). A solution of 4-benzyloxy-3-methoxybenzonitrile (3.50 g, 14.62 mmol) in acetic anhydride (40 mL) was cooled to 0 °C, and 69 wt % nitric acid (3.6 mL, 55 mmol) was added slowly. The reaction mixture was stirred overnight at room temperature and then poured into ice−water. The resulting precipitate was collected, washed with water, and dried to provide 4-benzyloxy-5-methoxy-2-nitrobenzonitrile. A mixture of crude 4-benzyloxy-5-methoxy-2-nitrobenzonitrile, iron dust (3.0 g, 54.8 mmol), and ammonium chloride (4.4 g, 82.2 mmol) in isopropyl alcohol−water (50:30 mL) was heated to reflux for 4 h. Then, the resulting mixture was filtered and washed with 5% methanol in dichloromethane (150 mL). The organic phase of the filtrate was dried, concentrated, and purified by silica gel chromatography (DCM to 10% MeOH in DCM) to afford 2-amino-4-benzyloxy-5-methoxybenzonitrile as a yellow solid (**5**, 2.68 g, 72% yield over 2 steps). ^{1}H NMR (400 MHz, MeOH-d_4) δ ppm 7.43−7.28 (m, 5H), 7.12 (s, 1H), 6.41 (s, 1H), 5.07 (s, 2H), 3.76 (s, 3H).

7-(Benzyloxy)-6-methoxyquinazoline-2,4($1H,3H$)-dione (6). Methyl chloroformate (0.94 mL, 12.1 mmol) was added into the solution of 2-amino-4-benzyloxy-5-methoxybenzonitrile (2.05 g, 8.06 mmol) and DIEA (2.6 mL, 16.1 mmol) in cosolvent DMF: DCM (20:10 mL) at 0 °C. The reaction solution was stirred overnight at room temperature, and then 60 mL of water was added. The resulting precipitate was collected, washed with water, dried, and used in the next step without further purification. A mixture of the product, 30 wt % H$_2$O$_2$ (20 mL), and NaOH (322 mg, 8.06 mmol) in ethanol (100 mL) was stirred for 2 h under reflux. After adding 100 mL of water, the reaction mixture was cooled to RT, and the resulting precipitate was collected, washed with water, and dried to afford compound **6** as a white solid (1.68 g, 70% yield over 2 steps). ^{1}H NMR (400 MHz, DMSO-d_6) δ ppm 11.03 (br, s, 2H), 7.48−7.36 (m, 5H), 7.28 (s, 1H), 6.78 (s, 1H), 5.14 (s, 2H), 3.79 (s, 3H). ^{13}C NMR (100 MHz, DMSO-d_6) δ ppm 162.8, 154.2, 150.8, 145.6, 136.8, 136.3, 128.9, 128.6, 128.5, 107.8, 106.8, 99.5, 70.5, 56.2. MS (ESI): 299 [M + H]$^+$.

7-(Benzyloxy)-2,4-dichloro-6-methoxyquinazoline (7). A mixture of compound **5** (1.95 g, 6.54 mmol) and N,N-diethylaniline (1.15 mL, 7.19 mmol) in POCl$_3$ (10 mL) was stirred for 7 h under reflux. The reaction mixture was concentrated in vacuo, and saturated sodium bicarbonate aqueous solution (20 mL) was added. The resulting mixture was extracted with chloroform (30 mL × 2). The combined organic phases were dried, filtered, concentrated, and purified by silica gel chromatography (hexanes to 20% ethyl acetate in hexanes) to afford compound **7** as a yellow solid (1.30 g, 59% yield). ^{1}H NMR (400 MHz, CDCl$_3$) δ ppm 7.39−7.27 (m, 5H), 7.25 (s, 1H), 7.19 (s, 1H), 5.21 (s, 2H), 3.97 (s, 3H).

7-(Benzyloxy)-6-methoxy-2-(4-methyl-1,4-diazepan-1-yl)-N-(1-methylpiperidin-4-yl)quinazolin-4-amine (8). A mixture of compound **7** (1.30 g, 3.88 mmol), 4-amino-1-methylpiperidine

(1.33 g, 11.64 mmol), and DIEA (0.96 mL, 5.82 mmol) in THF (10 mL) was stirred overnight at room temperature. After concentration in vacuo, the crude product was purified by silica gel chromatography (DCM to 10% MeOH in DCM) to afford 7-(benzyloxy)-2-chloro-6-methoxy-*N*-(1-methylpiperidin-4-yl)-quinazolin-4-amine as a yellow solid (1.60 g, 100% yield). ^{1}H NMR (400 MHz, CDCl$_3$) δ ppm 7.46−7.26 (m, 5H), 7.13 (s, 1H), 6.86 (s, 1H), 5.51 (d, *J* = 7.9 Hz, 1H), 5.22 (s, 2H), 4.42−4.22 (m, 1H), 3.99 (s, 3H), 2.97 (d, *J* = 11.9 Hz, 2H), 2.38 (s, 3H), 2.32 (td, *J* = 11.9, 2.2 Hz, 2H), 2.15 (d, *J* = 9.6 Hz, 2H), 1.81−1.71 (m, 2H). ^{13}C NMR (100 MHz, CDCl$_3$) δ 159.16, 156.07, 153.95, 149.30, 147.75, 135.48, 128.65, 128.18, 127.18, 108.66, 106.90, 100.25, 70.75, 56.36, 54.57, 47.98, 46.17, 32.11. MS (ESI): 413 [M + H]$^+$. Then, a mixture of 7-(benzyloxy)-2-chloro-6-methoxy-*N*-(1-me-thylpiperidin-4-yl)quinazolin-4-amine (1.31 g, 3.17 mmol), 1-methylhomopiperazine (0.80 mL, 6.35 mmol), and 4.0 M HCl in dioxane (1.6 mL, 6.4 mmol) in isopropyl alcohol was heated by microwave irradiation for 15 min to 160 °C in a sealed tube. The reaction mixture was diluted with 30 mL of DCM and washed with saturated sodium bicarbonate aqueous solution (10 mL). The organic phase was dried, filtered, concentrated, and purified by silica gel chromatography (DCM to 20% MeOH in DCM) to afford compound **8** as a yellow solid (1.30 g, 83% yield). ^{1}H NMR (400 MHz, MeOH-*d*$_4$) δ ppm 7.42 (s, 1H), 7.40−7.20 (m, 5H), 6.96 (s, 1H), 5.08 (s, 2H), 4.11−4.03 (m, 1H), 3.90−3.84 (m, 5H), 3.78 (t, *J* = 6.3 Hz, 2H), 2.93 (d, *J* = 12.1 Hz, 2H), 2.80−2.68 (m, 2H), 2.58 (dd, *J* = 6.4, 4.4 Hz, 2H), 2.34 (s, 3H), 2.29 (s, 3H), 2.17 (dd, *J* = 12.0, 10.1 Hz, 2H), 2.05 (d, *J* = 10.5 Hz, 2H), 2.00−1.94 (m, 2H), 1.75−1.65 (m, 2H). ^{13}C NMR (100 MHz, MeOH-*d*$_4$) δ 160.08, 158.83, 155.09, 147.93, 147.45, 137.98, 129.66, 129.15, 128.68, 106.64, 105.00, 104.60, 71.56, 59.50, 58.15, 57.06, 56.00, 49.47, 46.98, 46.67, 46.53, 46.23, 32.24, 28.30. MS (ESI): 491 [M + H]$^+$.

6-Methoxy-2-(4-methyl-1,4-diazepan-1-yl)-4-(1-methylpiperi-din-4-ylamino)quinazolin-7-ol (9). A mixture of compound **8** (1.29 g, 2.63 mmol), 1,4-cyclohexadiene (2.6 mL, 26 mmol), and 10 wt % Pd/C (400 mg) in ethanol (30 mL) was heated to reflux 2 h. The reaction mixture was filtered and concentrated to provide the debenzylated product **9** as a yellow solid, which was used without purification. MS (ESI): 401 [M + H]$^+$.

7-(3-(Dimethylamino)propoxy)-6-methoxy-2-(4-methyl-1,4-dia-zepan-1-yl)-*N*-(1-methylpiperidin-4-yl)quinazolin-4-amine (10). Under nitrogen gas, DIAD (250 μL, 1.25 mmol) was added into the ice-cooled mixture of compound **9** (100 mg, 0.250 mmol), 3-(dimethylamino)propan-1-ol (120 μL, 1.00 mmol), and PPh$_3$ (362 mg, 1.38 mmol) in THF (3.0 mL). The reaction mixture was stirred overnight at RT. After concentration in vacuo, the crude product was purified by preparative HPLC with a gradient from 10% of MeOH (A) in 0.1% TFA in H$_2$O (B) to 100% of MeOH (A). The resulting product was basified with a saturated solution of NaHCO$_3$ and extracted with CH$_2$Cl$_2$ to afford 56 mg of the desired product **10** as a white solid (46% yield over 2 steps). ^{1}H NMR (400 MHz, CDCl$_3$) δ ppm 6.87 (s, 1H), 6.71 (s, 1H), 4.96 (d, *J* = 7.0 Hz, 1H), 4.11 (t, *J* = 6.8 Hz, 2H), 4.08−3.98 (m, 1H), 3.94 (dd, *J* = 5.6, 4.0 Hz, 2H), 3.87 (s, 3H), 3.84 (t, *J* = 6.4 Hz, 2H), 2.83 (d, *J* = 11.8 Hz, 2H), 2.72−2.63 (m, 2H), 2.59−2.51 (m, 2H), 2.47−2.37 (m, 2H), 2.34 (s, 3H), 2.29 (s, 3H), 2.20 (s, 6H), 2.10−2.17 (m, 4H), 2.08−1.94 (m, 4H), 1.68−1.49 (m, 2H). ^{13}C NMR (100 MHz, CDCl$_3$) δ 158.52, 157.99, 153.91, 149.58, 145.15, 106.95, 102.67, 101.44, 67.14, 58.90, 57.30, 56.65, 56.25, 54.75, 47.87, 46.66, 46.25, 45.83, 45.43, 32.25, 27.81, 27.20. MS (ESI): 486 [M + H]$^+$. HPLC: 100%; RT: 0.765 min. HRMS calcd for C$_{26}$H$_{43}$N$_7$O$_2$: 485.3478. Found: 484.3410 [M − H].

7-(2-(Dimethylamino)ethoxy)-6-methoxy-2-(4-methyl-1,4-dia-zepan-1-yl)-*N*-(1-methylpiperidin-4-yl)quinazolin-4-amine (11). Compound **11** was prepared as a white solid from phenol **9** and 2-(dimethylamino)ethanol via Mitsunobu reaction (43% yield over 2 steps). ^{1}H NMR (400 MHz, CDCl$_3$) δ ppm 6.81 (s, 1H), 6.72 (s, 1H), 5.05 (d, *J* = 6.8 Hz, 1H), 4.09 (t, *J* = 6.0 Hz, 2H), 3.95−4.05 (m, 1H), 3.94−3.86 (m, 2H), 3.82−3.80 (m, 5H), 2.78

(d, *J* = 11.2 Hz, 2H), 2.72 (t, *J* = 6.0 Hz, 2H), 2.62 (t, *J* = 4.3 Hz, 2H), 2.53−2.45 (m, 2H), 2.29 (s, 3H), 2.24 (s, 9H), 2.08 (t, *J* = 9.3 Hz, 4H), 1.94 (dd, *J* = 10.5, 5.5 Hz, 2H), 1.53 (dd, *J* = 21.4, 10.6 Hz, 2H). ^{13}C NMR (100 MHz, CDCl$_3$) δ 158.58, 157.99, 153.65, 149.54, 145.07, 106.79, 102.82, 101.34, 66.57, 58.94, 57.83, 57.34, 56.38, 54.77, 47.96, 46.71, 46.26, 45.86, 45.84, 32.23, 27.89. HPLC: 99%, RT: 0.713 min. MS (ESI): 472 [M + H]$^+$.

7-(4-(Dimethylamino)butoxy)-6-methoxy-2-(4-methyl-1,4-dia-zepan-1-yl)-*N*-(1-methylpiperidin-4-yl)quinazolin-4-amine (12). Intermediate **30** was prepared from phenol **9** (117 mg, 0.292 mmol) and 4-chlorobutan-1-ol (127 mg, 1.17 mmol) and purified by basic alumina chromatography (DCM to 5% MeOH in DCM) to afford the crude product (95 mg). Then a mixture of **30**, dimethylamine (0.8 mL) and *i*-PrOH (2.5 mL) was stirred for 15 min at 160 °C in a microwave reactor. After purification (same as **10**), 17 mg of compound **12** was obtained as a yellow solid (12% yield over three steps). ^{1}H NMR (400 MHz, CDCl$_3$) δ ppm 6.80 (s, 1H), 6.65 (s, 1H), 4.87 (d, *J* = 6.9 Hz, 1H), 3.97−4.06 (m, 3H), 3.93−3.76 (m, 7H), 2.80 (d, *J* = 11.0 Hz, 2H), 2.68−2.58 (m, 2H), 2.55−2.45 (m, 2H), 2.31 (s, 3H), 2.28−2.22 (m, 5H), 2.16 (s, 6H), 2.10 (t, *J* = 11.1 Hz, 4H), 1.95 (dd, *J* = 14.9, 9.8 Hz, 2H), 1.89−1.78 (m, 2H), 1.65−1.48 (m, 4H). ^{13}C NMR (100 MHz, CDCl$_3$) δ 158.59, 158.00, 154.01, 149.65, 145.23, 106.86, 102.64, 101.47, 68.47, 59.37, 58.97, 57.35, 56.70, 54.78, 47.88, 46.71, 46.30, 45.87, 45.83, 45.47, 32.32, 27.88, 26.83, 24.23. HPLC: 100%; RT: 0.762 min. MS (ESI): 500 [M + H]$^+$.

7-(5-(Dimethylamino)pentyloxy)-6-methoxy-2-(4-methyl-1,4-diazepan-1-yl)-*N*-(1-methylpiperidin-4-yl)quinazolin-4-amine (13). Compound **13** was prepared as an off-white solid by the procedure as the preparation of compound **12** (28% yield over three steps). ^{1}H NMR (400 MHz, CDCl$_3$) δ 6.82 (s, 1H), 6.70 (s, 1H), 4.96 (d, *J* = 6.9 Hz, 1H), 4.04 (m, 3H), 3.97−3.90 (m, 2H), 3.89−3.78 (m, 5H), 2.82 (d, *J* = 11.3 Hz, 2H), 2.70−2.61 (m, 2H), 2.57−2.48 (m, 2H), 2.33 (s, 3H), 2.28 (s, 3H), 2.25−2.20 (m, 2H), 2.17 (s, 6H), 2.12 (t, *J* = 10.2 Hz, 4H), 1.97 (dd, *J* = 10.9, 5.5 Hz, 2H), 1.91−1.81 (m, 2H), 1.65−1.37 (m, 6H). ^{13}C NMR (100 MHz, CDCl$_3$) δ 158.59, 157.99, 153.95, 149.64, 145.16, 106.79, 102.63, 101.36, 68.60, 59.66, 58.96, 57.35, 56.60, 54.78, 47.90, 46.72, 46.29, 45.87, 45.84, 45.49, 32.29, 28.85, 27.89, 27.44, 23.88. HPLC: 100%; RT: 0.762 min. MS (ESI): 514 [M + H]$^+$.

7-(6-(Dimethylamino)ethoxy)-6-methoxy-2-(4-methyl-1,4-dia-zepan-1-yl)-*N*-(1-methylpiperidin-4-yl)quinazolin-4-amine (14). Compound **14** was prepared as a white solid from phenol **9** and 6-(dimethylamino)hexan-1-ol via Mitsunobu reaction (39% yield over 2 steps). ^{1}H NMR (400 MHz, CDCl$_3$) δ 6.81 (s, 1H), 6.71 (s, 1H), 4.99 (d, *J* = 6.9 Hz, 1H), 4.02 (m, 3H), 3.96−3.88 (m, 2H), 3.90−3.76 (m, 5H), 2.81 (d, *J* = 11.3 Hz, 2H), 2.69−2.60 (m, 2H), 2.57−2.45 (m, 2H), 2.32 (s, 3H), 2.26 (s, 3H), 2.23−2.03 (m, 12H), 1.96 (dd, *J* = 10.7, 5.5 Hz, 2H), 1.83 (dt, *J* = 14.2, 6.9 Hz, 2H), 1.56 (dd, *J* = 21.3, 10.7 Hz, 2H), 1.46−1.39 (m, 4H), 1.36−1.25 (m, 2H). ^{13}C NMR (100 MHz, CDCl$_3$) δ 158.57, 157.98, 153.94, 149.63, 145.13, 106.79, 102.61, 101.40, 68.63, 59.75, 58.94, 57.33, 56.58, 54.76, 47.90, 46.70, 46.27, 45.84, 45.47, 32.26, 28.83, 27.87, 27.61, 27.17, 25.91. HPLC: 100%, RT: 0.758 min. MS (ESI): 528 [M + H]$^+$.

6-Methoxy-2-(4-methyl-1,4-diazepan-1-yl)-7-(3-(methylamino)-propoxy)-*N*-(1-methylpiperidin-4-yl)quinazolin-4-amine (15). Compound **15** was prepared as an off-white solid from phenol **9** and 3-(methylamino)propan-1-ol via Mitsunobu reaction (33% yield over 2 steps). ^{1}H NMR (400 MHz, CD$_3$OD) δ 7.43 (s, 1H), 6.92 (s, 1H), 4.22−4.10 (m, 3H), 3.98−3.94 (m, 2H), 3.93 (s, 3H), 3.87 (t, *J* = 6.3 Hz, 2H), 2.99 (d, *J* = 11.8 Hz, 2H), 2.86 (t, *J* = 6.8 Hz, 2H), 2.80−2.74 (m, 2H), 2.65−2.60 (m, 2H), 2.47 (d, *J* = 0.9 Hz, 3H), 2.39 (s, 3H), 2.35 (s, 3H), 2.22 (t, *J* = 11.8 Hz, 2H), 2.12−2.02 (m, 6H), 1.76 (dd, *J* = 21.1, 12.0 Hz, 2H). ^{13}C NMR (100 MHz, CD$_3$OD) δ 160.27, 160.16, 155.10, 150.02, 147.01, 106.80, 105.04, 104.28, 68.62, 59.84, 58.25, 57.02, 56.22, 50.20, 46.90, 46.79, 46.72, 46.41, 35.99, 32.52, 29.43, 28.61. HPLC: 99%, RT 0.513 min. MS (ESI): 472 [M + H]$^+$.

7-(3-(Diethylamino)propoxy)-6-methoxy-2-(4-methyl-1,4-dia-zepan-1-yl)-*N*-(1-methylpiperidin-4-yl)quinazolin-4-amine (16).

Compound **16** was prepared as a yellow solid from phenol **9** and 3-(diethylamino)propan-1-ol via Mitsunobu reaction (47% yield over 2 steps). ^{1}H NMR (400 MHz, CD₃OD) δ 7.42 (s, 1H), 6.92 (s, 1H), 4.19−4.11 (m, 3H), 3.99−3.93 (m, 2H), 3.91 (s, 3H), 3.87 (t, *J* = 6.3 Hz, 2H), 2.99 (d, *J* = 12.0 Hz, 2H), 2.80−2.70 (m, 4H), 2.67−2.59 (m, 6H), 2.39 (s, 3H), 2.35 (s, 3H), 2.21 (t, *J* = 12.0 Hz, 2H), 2.13 (d, *J* = 11.9 Hz, 2H), 2.08−1.98 (m, 4H), 1.74 (dt, *J* = 12.6, 8.2 Hz, 2H), 1.11 (t, *J* = 7.0 Hz, 6H). ^{13}C NMR (100 MHz, CD₃OD) δ 160.26, 160.16, 155.30, 150.07, 147.09, 106.84, 104.96, 104.46, 68.11, 59.85, 58.25, 57.06, 56.22, 50.41, 48.02, 46.91, 46.79, 46.72, 46.41, 32.53, 28.61, 26.93, 11.56. HPLC: 99%, RT 0.525 min. MS (ESI): 514 [M + H]⁺.

6-Methoxy-7-(3-(methyl(propyl)amino)propoxy)-2-(4-methyl-1,4-diazepan-1-yl)-*N*-(1-methylpiperidin-4-yl)quinazolin-4-amine (17). Compound **17** was prepared as a yellow solid from phenol **9** by the same general procedure as described for the preparation of compound **12** (50% yield over three steps). ^{1}H NMR (400 MHz, CDCl₃) δ 6.86 (s, 1H), 6.70 (s, 1H), 4.93 (d, *J* = 6.9 Hz, 1H), 4.11 (t, *J* = 6.7 Hz, 2H), 4.08−3.99 (m, 1H), 3.99−3.90 (m, 2H), 3.90−3.78 (m, 5H), 2.84 (d, *J* = 11.5 Hz, 2H), 2.70−2.63 (m, 2H), 2.58−2.51 (m, 2H), 2.48 (t, *J* = 7.1 Hz, 2H), 2.34 (s, 3H), 2.31−2.23 (m, 5H), 2.19 (s, 3H), 2.13 (t, *J* = 10.1 Hz, 4H), 2.06−1.93 (m, 4H), 1.59 (dd, *J* = 21.1, 11.0 Hz, 2H), 1.45 (dq, *J* = 14.8, 7.4 Hz, 2H), 0.85 (t, *J* = 7.4 Hz, 3H). ^{13}C NMR (100 MHz, CDCl₃) δ 158.57, 158.00, 154.01, 149.66, 145.19, 106.97, 102.66, 101.47, 67.24, 59.72, 58.96, 57.35, 56.69, 54.78, 54.15, 47.90, 46.71, 46.30, 45.86, 42.22, 32.31, 27.87, 26.84, 20.46, 11.90. HPLC: 100%; RT: 0.759 min. MS (ESI): 514 [M + H]⁺.

6-Methoxy-2-(4-methyl-1,4-diazepan-1-yl)-*N*-(1-methylpiperidin-4-yl)-7-(3-(pyrrolidin-1-yl)propoxy)quinazolin-4-amine (18). Compound **18** was prepared as a white solid from phenol **9** by the same general procedure as described for the preparation of compound **12** (48% yield over three steps). ^{1}H NMR (400 MHz, CDCl₃) δ 6.87 (s, 1H), 6.71 (s, 1H), 4.95 (d, *J* = 6.6 Hz, 1H), 4.14 (t, *J* = 6.7 Hz, 2H), 4.10−3.99 (m, 1H), 3.98−3.90 (m, 2H), 3.90−3.79 (m, 5H), 2.84 (d, *J* = 10.5 Hz, 2H), 2.66 (d, *J* = 3.9 Hz, 2H), 2.64−2.42 (m, 8H), 2.34 (s, 3H), 2.29 (s, 3H), 2.21−2.02 (m, 6H), 2.03−1.91 (m, 2H), 1.83−1.69 (m, 4H), 1.59 (dd, *J* = 21.6, 11.1 Hz, 2H). ^{13}C NMR (100 MHz, CDCl₃) δ 158.53, 157.99, 153.96, 149.61, 145.15, 106.95, 102.65, 101.47, 67.28, 58.93, 57.32, 56.66, 54.76, 54.14, 52.91, 47.88, 46.69, 46.27, 45.84, 32.28, 28.50, 27.84, 23.44. HPLC: 100%; RT: 0.761 min. MS (ESI): 512 [M + H]⁺.

6-Methoxy-2-(4-methyl-1,4-diazepan-1-yl)-*N*-(1-methylpiperidin-4-yl)-7-(3-(piperidin-1-yl)propoxy)quinazolin-4-amine (19). Compound **19** was prepared as a white solid from phenol **9** and 1-piperidinepropanol via Mitsunobu reaction (36% yield over 2 steps). ^{1}H NMR (400 MHz, CDCl₃) δ 6.87 (s, 1H), 6.69 (s, 1H), 4.92 (d, *J* = 6.9 Hz, 1H), 4.12 (t, *J* = 6.6 Hz, 2H), 4.05 (dd, *J* = 14.2, 8.5 Hz, 1H), 3.99−3.91 (m, 2H), 3.91−3.79 (m, 5H), 2.84 (d, *J* = 11.4 Hz, 2H), 2.72−2.63 (m, 2H), 2.60−2.50 (m, 2H), 2.44 (t, *J* = 7.1 Hz, 2H), 2.35 (m, 7H), 2.30 (s, 3H), 2.14 (t, *J* = 10.0 Hz, 4H), 2.08−1.92 (m, 4H), 1.66−1.50 (m, 6H), 1.47−1.35 (m, 2H). ^{13}C NMR (100 MHz, CDCl₃) δ 158.57, 157.98, 154.00, 149.65, 145.18, 106.96, 102.63, 101.46, 67.41, 58.95, 57.34, 56.69, 55.76, 54.76, 54.56, 47.86, 46.70, 46.28, 45.85, 45.83, 32.30, 27.86, 26.48, 25.98, 24.44. HPLC: 99%; RT: 0.713 min. MS (ESI): 526 [M + H]⁺.

6-Methoxy-2-(4-methyl-1,4-diazepan-1-yl)-*N*-(1-methylpiperidin-4-yl)-7-(3-morpholinopropoxy)quinazolin-4-amine (20). Compound **20** was prepared as a white solid from phenol **9** and 3-morpholinopropan-1-ol via Mitsunobu reaction (38% yield over 2 steps). ^{1}H NMR (400 MHz, CDCl₃) δ 6.88 (s, 1H), 6.69 (s, 1H), 4.91 (d, *J* = 6.7 Hz, 1H), 4.15 (t, *J* = 6.6 Hz, 2H), 4.09−4.02 (m, 1H), 3.94 (d, *J* = 4.1 Hz, 2H), 3.89 (s, 3H), 3.85 (t, *J* = 6.3 Hz, 2H), 3.75−3.64 (m, 4H), 2.84 (d, *J* = 10.8 Hz, 2H), 2.67 (d, *J* = 3.9 Hz, 2H), 2.58−2.37 (m, 8H), 2.33 (d, *J* = 13.6 Hz, 3H), 2.30 (s, 3H), 2.13 (d, *J* = 10.4 Hz, 4H), 2.03 (td, *J* = 13.9, 6.1 Hz, 4H), 1.59 (dd, *J* = 21.4, 10.4 Hz, 2H). ^{13}C NMR (100 MHz, CDCl₃) δ 157.63, 157.00, 152.91, 148.69, 144.15, 106.00, 101.70, 100.38,

66.01, 57.97, 56.38, 55.66, 54.35, 53.79, 52.70, 46.92, 45.74, 45.31, 44.89, 31.34, 28.68, 26.91, 25.10. HPLC: 99%; RT: 0.762 min. MS (ESI): 528 [M + H]⁺.

6-Methoxy-2-(4-methyl-1,4-diazepan-1-yl)-7-(4-methylpentyloxy)-*N*-(1-methylpiperidin-4-yl)quinazolin-4-amine (21). Compound **21** was prepared as a white solid from phenol **9** and 4-methylpentan-1-ol via Mitsunobu reaction (45% yield over 2 steps). ^{1}H NMR (400 MHz, CD₃OD) δ 7.41 (s, 1H), 6.89 (s, 1H), 4.12 (ddd, *J* = 11.4, 9.8, 3.8 Hz, 1H), 4.04 (t, *J* = 6.5 Hz, 2H), 3.96−3.88 (m, 5H), 3.84 (t, *J* = 6.3 Hz, 2H), 2.95 (d, *J* = 11.6 Hz, 2H), 2.78−2.70 (m, 2H), 2.63−2.55 (m, 2H), 2.36 (s, 3H), 2.32 (s, 3H), 2.18 (t, *J* = 11.9 Hz, 2H), 2.10 (d, *J* = 12.0 Hz, 2H), 2.05−1.97 (m, 2H), 1.88−1.79 (m, 2H), 1.78−1.66 (m, 2H), 1.61 (td, *J* = 13.2, 6.6 Hz, 1H), 1.41−1.32 (m, 2H), 0.93 (d, *J* = 6.6 Hz, 6H). ^{13}C NMR (100 MHz, CD₃OD) δ 160.21, 160.03, 155.44, 149.97, 147.07, 106.63, 104.82, 104.43, 70.14, 59.85, 58.24, 57.05, 56.20, 46.92, 46.78, 46.69, 46.41, 36.46, 32.51, 29.21, 28.59, 28.19, 23.12. HPLC: 99%; RT 2.570 min. MS (ESI): 485 [M + H]⁺.

6-Methoxy-7-(4-methoxybutoxy)-2-(4-methyl-1,4-diazepan-1-yl)-*N*-(1-methylpiperidin-4-yl)quinazolin-4-amine (22). Compound **22** was prepared as an off-white solid from phenol **9** and 4-methoxybutan-1-ol via Mitsunobu reaction (38% yield over 2 steps). ^{1}H NMR (400 MHz, CDCl₃) δ 6.84 (s, 1H), 6.71 (s, 1H), 4.96 (d, *J* = 7.0 Hz, 1H), 4.12−3.99 (m, 3H), 3.93 (dd, *J* = 5.7, 4.0 Hz, 2H), 3.86 (s, 3H), 3.84 (t, *J* = 6.4 Hz, 2H), 3.40 (t, *J* = 6.4 Hz, 2H), 3.30 (s, 3H), 2.83 (d, *J* = 11.8 Hz, 2H), 2.69−2.63 (m, 2H), 2.53 (dd, *J* = 6.5, 4.4 Hz, 2H), 2.33 (s, 3H), 2.28 (s, 3H), 2.20−2.07 (m, 4H), 2.04−1.86 (m, 4H), 1.79−1.67 (m, 2H), 1.66−1.50 (m, 2H). ^{13}C NMR (100 MHz, CDCl₃) δ 158.58, 157.99, 153.92, 149.62, 145.18, 106.82, 102.65, 101.46, 72.24, 68.34, 58.94, 58.52, 57.34, 56.63, 54.77, 47.88, 46.70, 46.27, 45.85, 45.82, 32.27, 27.87, 26.15, 25.67. HPLC: 99%; RT 0.700 min. MS (ESI): 487 [M + H]⁺.

***tert*-Butyl 4-(6-Methoxy-2-(4-methyl-1,4-diazepan-1-yl)-4-(1-methylpiperidin-4-ylamino)quinazolin-7-yloxy)butylcarbamate (23).** Compound **23** was prepared as a white solid from phenol **9** and *tert*-butyl 4-hydroxybutylcarbamate via Mitsunobu reaction (45% yield over 2 steps). ^{1}H NMR (400 MHz, CDCl₃) δ 6.82 (s, 1H), 6.69 (s, 1H), 4.93−4.82 (m, 2H), 4.15−4.00 (m, 3H), 3.96−3.93 (m, 2H), 3.91 (s, 3H), 3.85 (t, *J* = 6.1 Hz, 2H), 3.23−3.10 (m, 2H), 2.85 (d, *J* = 11.4 Hz, 2H), 2.72−2.62 (m, 2H), 2.61−2.51 (m, 2H), 2.35 (s, 3H), 2.31 (s, 3H), 2.15 (t, *J* = 9.5 Hz, 4H), 2.04−1.84 (m, 4H), 1.72−1.53 (m, 4H), 1.43 (s, 9H). HPLC: 99%, RT 0.703 min. MS (ESI): 572 [M + H]⁺.

7-(5-Aminopentyloxy)-6-methoxy-2-(4-methyl-1,4-diazepan-1-yl)-*N*-(1-methylpiperidin-4-yl)quinazolin-4-amine (24). Compound **24** was prepared as a white solid from phenol **9** and *tert*-butyl 5-hydroxypentylcarbamate via Mitsunobu reaction, followed by the deprotection of the Boc group by TFA (34% yield over three steps). ^{1}H NMR (400 MHz, CDCl₃) δ 6.82 (s, 1H), 6.71 (s, 1H), 4.09−3.97 (m, 3H), 3.92 (d, *J* = 4.1 Hz, 2H), 3.89−3.77 (m, 5H), 2.82 (d, *J* = 10.9 Hz, 2H), 2.64 (m, 4H), 2.51 (d, *J* = 5.0 Hz, 2H), 2.32 (s, 3H), 2.27 (s, 3H), 2.16−2.09 (m, 4H), 2.03−1.90 (m, 2H), 1.90−1.79 (m, 2H), 1.57 (dd, *J* = 21.3, 10.3 Hz, 2H), 1.45 (m, 4H). ^{13}C NMR (100 MHz, CDCl₃) δ 158.60, 157.94, 153.88, 149.63, 145.12, 106.79, 102.61, 101.39, 68.54, 58.94, 57.35, 56.57, 54.77, 47.79, 46.71, 46.27, 45.85, 41.82, 33.43, 32.23, 28.72, 27.88, 23.28. HPLC: 99%; RT 0.539 min. MS (ESI): 486 [M + H]⁺.

5-(6-Methoxy-2-(4-methyl-1,4-diazepan-1-yl)-4-(1-methylpiperidin-4-ylamino)quinazolin-7-yloxy)pentanamide (25). Compound **25** was prepared as a yellow solid from phenol **9** and 5-hydroxypentanamide via Mitsunobu reaction (17% yield over 2 steps). ^{1}H NMR (400 MHz, CD₃OD) δ 7.40 (s, 1H), 6.89 (s, 1H), 4.13 (m, 3H), 3.95−3.90 (m, 2H), 3.89 (s, 3H), 3.84 (t, *J* = 6.4 Hz, 2H), 2.96 (d, *J* = 12.0 Hz, 2H), 2.79−2.70 (m, 2H), 2.60 (dd, *J* = 6.5, 4.4 Hz, 2H), 2.36 (s, 3H), 2.34−2.29 (m, 5H), 2.25−2.14 (m, 2H), 2.10 (d, *J* = 12.2 Hz, 2H), 2.06−1.97 (m, 2H), 1.95−1.66 (m, 6H). ^{13}C NMR (100 MHz, CD₃OD) δ 177.43, 158.64, 158.50, 153.69, 148.40, 145.39, 105.05, 103.29, 102.75, 68.03, 58.25, 56.65, 55.40, 54.61, 45.32, 45.19, 45.11, 44.81, 34.68, 30.92, 27.91, 27.00, 22.41. HPLC: 99%; RT 0.692 min. MS (ESI): 500 [M + H]⁺.

6-Methoxy-2-(4-methyl-1,4-diazepan-1-yl)-*N*-(1-methylpiperidin-4-yl)-7-(2-(2-(pyrrolidin-1-yl)ethoxy)ethoxy)quinazolin-4-amine (26). Compound **26** was prepared as a yellow solid from phenol **9** and 2-(2-(pyrrolidin-1-yl)ethoxy)ethanol via Mitsunobu reaction (49% yield over 2 steps). ^{1}H NMR (400 MHz, CDCl$_3$) δ 6.83 (s, 1H), 6.73 (s, 1H), 5.06 (d, J = 6.9 Hz, 1H), 4.19 (t, J = 5.0 Hz, 2H), 4.09−3.96 (m, 1H), 3.95−3.88 (m, 2H), 3.88−3.76 (m, 7H), 3.62 (t, J = 6.0 Hz, 2H), 2.81 (d, J = 11.5 Hz, 2H), 2.63 (t, J = 5.9 Hz, 4H), 2.53−2.47 (m, 6H), 2.31 (s, 3H), 2.26 (s, 3H), 2.10 (t, J = 10.1 Hz, 4H), 2.01−1.92 (m, 2H), 1.78−1.65 (m, 4H), 1.64−1.50 (m, 2H). ^{13}C NMR (100 MHz, CDCl$_3$) δ 158.51, 158.01, 153.64, 149.40, 145.12, 106.87, 102.93, 101.58, 70.41, 69.00, 67.85, 58.90, 57.31, 56.47, 55.50, 54.77, 54.53, 47.94, 46.67, 46.23, 45.84, 45.78, 32.19, 27.82, 23.38. HPLC: 99%; RT 0.549 min. MS (ESI): 542 [M + H]$^+$.

N^1-(2-(6-Methoxy-2-(4-methyl-1,4-diazepan-1-yl)-4-(1-methylpiperidin-4-ylamino)quinazolin-7-yloxy)ethyl)-N^1,N^2,N^2-trimethylethane-1,2-diamine (27). Compound **27** was prepared as a yellow solid from phenol **9** and 2-((2-(dimethylamino)ethyl)(methyl)amino)ethanol via Mitsunobu reaction (29% yield over 2 steps). ^{1}H NMR (400 MHz, CDCl$_3$) δ 6.86 (s, 1H), 6.68 (s, 1H), 4.91 (d, J = 6.7 Hz, 1H), 4.18 (t, J = 6.1 Hz, 2H), 4.12−3.99 (m, 1H), 3.95 (d, J = 4.3 Hz, 2H), 3.88−3.84 (m, 5H), 2.92 (t, J = 6.1 Hz, 2H), 2.85 (d, J = 11.1 Hz, 2H), 2.72−2.63 (m, 2H), 2.62−2.53 (m, 4H), 2.42 (t, J = 6.9 Hz, 2H), 2.35 (s, 6H), 2.30 (s, 3H), 2.23 (s, 6H), 2.15 (t, J = 10.2 Hz, 4H), 2.04−1.90 (m, 2H), 1.60 (dd, J = 21.1, 10.6 Hz, 2H). ^{13}C NMR (100 MHz, CDCl$_3$) δ 158.50, 157.97, 153.78, 149.48, 145.20, 106.83, 102.74, 101.23, 66.59, 58.91, 57.35, 57.31, 56.54, 56.20, 55.93, 54.75, 47.88, 46.67, 46.27, 45.82, 45.79, 45.76, 43.09, 32.29, 27.79. HPLC: 99%; RT 0.727 min. MS (ESI): 529 [M + H]$^+$.

6-Methoxy-2-(4-methyl-1,4-diazepan-1-yl)-*N*-(1-methylpiperidin-4-yl)-7-(piperidin-3-ylmethoxy)quinazolin-4-amine (28). Compound **28** was prepared as a white solid from phenol **9** and 3-piperidinemethanol via Mitsunobu reaction (40% yield over 2 steps). ^{1}H NMR (400 MHz, CDCl$_3$) δ 6.81 (s, 1H), 6.71 (s, 1H), 4.94 (d, J = 7.0 Hz, 1H), 4.08−3.99 (m, 1H), 3.97−3.90 (m, 2H), 3.90−3.78 (m, 7H), 3.23 (dd, J = 12.0, 2.7 Hz, 1H), 2.98 (d, J = 12.0 Hz, 1H), 2.82 (d, J = 11.6 Hz, 2H), 2.72−2.62 (m, 2H), 2.61−2.48 (m, 3H), 2.48−2.36 (m, 1H), 2.33 (s, 3H), 2.28 (s, 3H), 2.21−2.01 (m, 5H), 2.01−1.93 (m, 2H), 1.89 (d, J = 9.5 Hz, 1H), 1.81 (br, 1H), 1.70−1.38 (m, 4H), 1.20 (ddd, J = 24.4, 12.1, 3.8 Hz, 1H). ^{13}C NMR (100 MHz, CDCl$_3$) δ 158.59, 157.99, 154.14, 149.70, 145.24, 106.98, 102.70, 101.96, 71.77, 58.96, 57.35, 56.89, 54.77, 50.12, 47.90, 46.98, 46.73, 46.31, 45.87, 36.77, 32.31, 27.99, 27.90, 26.03. HPLC: 99%; RT 0.763 min. MS (ESI): 498 [M + H]$^+$.

7-(2-(2-(Dimethylamino)ethoxy)ethoxy)-6-methoxy-2-(4-methyl-1,4-diazepan-1-yl)-*N*-(1-methylpiperidin-4-yl)quinazolin-4-amine (29). Compound **29** was prepared as an off-white solid from phenol **9** and 2-(2-(dimethylamino)ethoxy)ethanol via Mitsunobu reaction (44% yield over 2 steps). ^{1}H NMR (400 MHz, CDCl$_3$) δ 6.80 (s, 1H), 6.72 (s, 1H), 5.02 (d, J = 6.9 Hz, 1H), 4.17 (t, J = 5.0 Hz, 2H), 4.01 (qd, J = 13.7, 8.3 Hz, 1H), 3.93−3.86 (m, 2H), 3.85−3.74 (m, 7H), 3.56 (t, J = 5.8 Hz, 2H), 2.79 (d, J = 11.2 Hz, 2H), 2.67−2.57 (m, 2H), 2.53−2.45 (m, 2H), 2.43 (t, J = 5.8 Hz, 2H), 2.30 (s, 3H), 2.24 (s, 3H), 2.18 (s, 6H), 2.08 (t, J = 9.0 Hz, 4H), 1.96−1.88 (m, 2H), 1.53 (dd, J = 21.4, 10.4 Hz, 2H). ^{13}C NMR (100 MHz, CDCl$_3$) δ 158.57, 157.98, 153.62, 149.54, 145.06, 106.95, 102.92, 101.59, 69.50, 68.99, 67.87, 58.93, 58.74, 57.33, 56.47, 54.77, 47.94, 46.71, 46.27, 45.84, 45.81, 32.23, 27.88. HPLC: 100%; RT 0.759 min. MS (ESI): 516 [M + H]$^+$.

Biochemical Assays General Procedures. The G9a enzyme used in the following assays was cloned and purified in Structural Genomics Consortium (SGC) [Mammalian Gene Collection; MGC AU80-H7 (BC018718)]. The construct amino acid sequence is from 913 to 1193.

ECSD Assay Experimental Procedures. The methyltransferase activity of PKMTs were measured using a coupled assay.[32] In this assay SAHH (*S*-adenosylhomocysteine hydrolase) and adenosine deaminase convert the methyltransferase reaction product SAH to homocysteine and inosine. The abundance of homocysteine can be quantified using ThioGlo (Calbiochem), which reacts with thiols and fluoresces strongly. The substrate peptide used in this assay was the first 25 residues of histone 3 [H3 (1−25)]. The SAHH clone was provided by Dr. Raymond Trievel (University of Michigan). For IC$_{50}$ determination, assay mixtures were prepared with 5 μM SAHH, about 0.3 U/mL of adenosine deaminase from Sigma, 16 μM SAM, 25 nM G9a, and 15 μM Thioglo. The inhibitors were added at concentrations ranging from 6 nM to 25 μM. After 5 min incubation, reactions were initiated by the addition of 5 μM H3 (1−25) peptide. The methylation reaction was followed by monitoring the increase in fluorescence using BioTek Synergy2 plate reader with 360/40 nm excitation filter and 528/20 nm emission filter for 20 min in 384 well-plate format. Homocysteine generated in the assay was quantitated using standard curves. Activity values were corrected by subtracting background caused by the peptide and the protein. IC$_{50}$ values were calculated using four parameter logistic equation by Sigmaplot software. Standard deviations were calculated from two independent experiments.

CLOT Assay Experimental Procedures. Substrate peptide b-H3(1−11) (biotin-ARTKQTARKST) was synthesized, HPLC-purified, and mass-analyzed by the Tufts Medical School Department of Physiology Core Facility (Boston, MA). To each well of a 1536-well white solid-bottom plate (Greiner Bio-One, Monroe, NC), 3 μL of G9a enzyme (final 7.5 nM) in PBS buffer, pH 7.4, containing 0.01% Tween-20 were added using a BioRAPTR (Beckman Coulter, Fullerton, CA) flying reagent dispenser (FRD). Compounds in DMSO (23 nL) were transferred to the assay plate with a Kalypsys pintool and assayed in duplicate in a 12-point dilution series, yielding a final concentration range of 32 pM to 57 μM and 0.5% DMSO. Following a 15 min incubation of compound with enzyme, b-H3(1−11) peptide and SAM substrates (final 500 nM and 20 μM, respectively) were added in a 1 μL FRD dispense. Reactions were incubated for 2 h at room temperature. To detect methylated b-H3(1−11) peptide, 0.5 μg/mL rabbit *anti*-methyllysine histone H3K9 antibody (Abcam Inc., Cambridge, MA) was added with 15 μg/mL streptavidin-coated donor and *anti*-rabbit IgG acceptor AlphaScreen (PerkinElmer, Waltham, MA) beads in a 1 μL FRD dispense. Following a 20 min incubation in the dark, plates were read on an EnVision multilabel plate reader (PerkinElmer) using the 1536 Plate HTS AlphaScreen aperture (80 ms excitation time, 240 ms measurement time). Data were normalized to no-enzyme and no-compound controls and dose−response curves were constructed. IC$_{50}$ values were determined with in-house curve fitting software using a four-parameter Hill equation as previously described (http://www.ncgc.nih.gov/pub/openhts/curvefit/).

DSF Experimental Procedures. A real-time PCR device (RTPCR 480 II) from Roche was used to monitor protein unfolding by monitoring the increase in the fluorescence of the fluorophor SYPRO Orange (Invitrogen, Carlsbad, CA) as described before.[39,40] Protein samples at 0.1 mg/mL in 100 mM Hepes buffer (pH 7.5) containing 150 mM NaCl, and 0, 6.25, 12.5, 25, 50, 100, and 200 μM of compounds were screened in the presence and absence of 500 μM SAH. Compound dilutions were made from stock solutions of 100% DMSO. The final concentration of DMSO was kept at 0.2% throughout the dilutions. All these solutions contained 5× Sypro Orange. Twenty μL aliquots were transferred to a 384-well PCR plate and scanned at a heating rate of 1 °C/min from 20 to 95 °C. Fluorescence intensities were plotted as a function of temperature by using an internally developed software package.[40]

Peptide Displacement Experimental Procedures. Fluorescence polarization measurements were performed in 384-well plates, using Synergy 2 microplate reader from BioTek.[41] The H3 (1−15) peptide (ARTKQTARKSTGGKA) was synthesized, N-terminally labeled with fluorescein [F−H3 (1−15)] and purified by Tufts University Core Services (Boston, MA). Displacement of the F−H3 (1−15) peptide was carried out using the

fluorescence polarization signal obtained upon peptide binding to G9a protein. Five μM of G9a was incubated with 36 nM peptide, and different concentrations of **3a**, **10**, or unlabeled H3 (1−25) from 0.5 to 500 μM were added. Displacement of the peptide was monitored by following the decrease in FP signal. Data were plotted and fit to a hyperbolic function using Sigma Plot software.

ITC Experimental Procedures. ITC measurements were performed in duplicate at 25 °C, using a VP-ITC microcalorimeter (MicroCal Inc.). Experiments were performed by injecting 10 μL of 300 μM solution of the compound **3a** or **10** into a sample cell containing 25 μM G9a that was extensively dialyzed in ITC buffer (25 mM Tris-HCl, pH 7.5, 200 mM NaCl, and 2 mM β-mercaptoethanol) and degassed. A total of 25 injections were performed with a spacing of 180 s and a reference power of 13 μcal/s. The ITC experiments were carried out in the presence of 500 μM SAH by adding it to both G9a and final solution of compounds. Compounds were first dissolved in 100% DMSO at 100 mM and were diluted in ITC buffer (final concentration of 0.3%). The concentration of DMSO was adjusted to 0.3% for the G9a solution. Heat of dilution generated by compounds was subtracted, and binding isotherms were plotted and analyzed using Origin Software (MicroCal Inc.). The ITC measurements were fit to a one-site binding model.

Morrison K_i Determination Using the Endoproteinase-coupled MCE Assay. The test compounds were titrated in 10% DMSO in 1X assay buffer (20 mM Tris-HCl pH = 8, 25 mM NaCl, 2 mM DTT and 0.025% Tween 20) using a 1.5-fold dilution scheme over 16 points. The compounds (5 μL) were then spotted into the assay wells of a 384-well microplate in triplicate. In the final assay volume of 50 μL, the compounds spanned a concentration range of 100 nM to 228 pM, and DMSO was 1%. A cocktail made in 1X assay buffer containing G9a (12.5 nM) and an H3K9 (5 μM) substrate peptide, ARTKme1QTARKSTGGK-5/6-FAM, where Kme1 indicates the presence of a monomethyl lysine and 5/6-FAM is a carboxyfluorescein tracer attached to the terminal lysine, was added and allowed to preincubate with the compounds for 10 min at 25 °C. The methyltransferase reaction was initiated by the addition of 10 μM SAM and allowed to proceed for 20 min at 25 °C, and then 10 μL of Endo-LysC (40 pg/μL) was added to proteolyze the remaining unmethylated peptide. Maximum and minimum signal controls were performed in the presence of 1% DMSO, and the minimum signal control reactions were initiated with 1X assay buffer rather than SAM. After 1 h, the plate was read on a Caliper Life Sciences EZ Reader II using upstream voltage −500 V, downstream voltage −1200 V, and pressure of −1.5 psi. The fractional velocities of the reactions were calculated and fit to a quadratic equation described by Morrison and co-workers[36,37] using a fixed enzyme concentration of 12.5 nM, a fixed substrate concentration of 5 μM, and a K_m of 31 μM for the peptide.

Supporting Information Available: ^{1}H and ^{13}C NMR spectra of compounds **10** and **29**. This material is available free of charge via the Internet at http://pubs.acs.org.

References

(1) Bernstein, B. E.; Meissner, A.; Lander, E. S. The mammalian epigenome. *Cell* **2007**, *128*, 669–681.

(2) Gelato, K. A.; Fischle, W. Role of histone modifications in defining chromatin structure and function. *Biol. Chem.* **2008**, *389*, 353–363.

(3) Strahl, B. D.; Allis, C. D. The language of covalent histone modifications. *Nature* **2000**, *403*, 41–45.

(4) Jenuwein, T.; Allis, C. D. Translating the histone code. *Science* **2001**, *293*, 1074–1080.

(5) Esteller, M. Epigenetics in cancer. *N. Engl. J. Med.* **2008**, *358*, 1148–1159.

(6) Lyko, F.; Brown, R. DNA methyltransferase inhibitors and the development of epigenetic cancer therapies. *J. Natl. Cancer Inst.* **2005**, *97*, 1498–1506.

(7) Martin, C.; Zhang, Y. The diverse functions of histone lysine methylation. *Nature Rev. Mol. Cell. Biol.* **2005**, *6*, 838–849.

(8) Rea, S.; Eisenhaber, F.; O'Carroll, D.; Strahl, B. D.; Sun, Z. W.; Schmid, M.; Opravil, S.; Mechtler, K.; Ponting, C. P.; Allis, C. D.; Jenuwein, T. Regulation of chromatin structure by site-specific histone H3 methyltransferases. *Nature* **2000**, *406*, 593–599.

(9) Kouzarides, T. Chromatin modifications and their function. *Cell* **2007**, *128*, 693–705.

(10) Copeland, R. A.; Solomon, M. E.; Richon, V. M. Protein methyltransferases as a target class for drug discovery. *Nature Rev. Drug Discovery* **2009**, *8*, 724–732.

(11) Spannhoff, A.; Sippl, W.; Jung, M. Cancer treatment of the future: inhibitors of histone methyltransferases. *Int. J. Biochem. Cell Biol.* **2009**, *41*, 4–11.

(12) Fog, C. K.; Jensen, K. T.; Lund, A. H. Chromatin-modifying proteins in cancer. *Acta Pathol., Microbiol. Immunol.* **2007**, *115*, 1060–1089.

(13) Spannhoff, A.; Hauser, A. T.; Heinke, R.; Sippl, W.; Jung, M. The emerging therapeutic potential of histone methyltransferase and demethylase inhibitors. *ChemMedChem* **2009**, *4*, 1568–1582.

(14) Li, Y.; Reddy, M. A.; Miao, F.; Shanmugam, N.; Yee, J.-K.; Hawkins, D.; Ren, B.; Natarajan, R. Role of the Histone H3 Lysine 4 Methyltransferase, SET7/9, in the Regulation of NF-{kappa}B-dependent Inflammatory Genes: Relevance to Diabetes and Inflammation. *J. Biol. Chem.* **2008**, *283*, 26771–26781.

(15) Maze, I.; Covington, H. E., III; Dietz, D. M.; LaPlant, Q.; Renthal, W.; Russo, S. J.; Mechanic, M.; Mouzon, E.; Neve, R. L.; Haggarty, S. J.; Ren, Y.; Sampath, S. C.; Hurd, Y. L.; Greengard, P.; Tarakhovsky, A.; Schaefer, A.; Nestler, E. J. Essential role of the histone methyltransferase G9a in cocaine-induced plasticity. *Science* **2010**, *327*, 213–216.

(16) Schaefer, A.; Sampath, S. C.; Intrator, A.; Min, A.; Gertler, T. S.; Surmeier, D. J.; Tarakhovsky, A.; Greengard, P. Control of Cognition and Adaptive Behavior by the GLP/G9a Epigenetic Suppressor Complex. *Neuron* **2009**, *64*, 678–691.

(17) Imai, K.; Togami, H.; Okamoto, T. Involvement of histone H3 Lysine 9 (H3K9) methyl transferase G9a in the maintenance of HIV-1 latency and its reactivation by BIX01294. *J. Biol. Chem.* **2010**, *285*, 16538–16545.

(18) Tachibana, M.; Sugimoto, K.; Nozaki, M.; Ueda, J.; Ohta, T.; Ohki, M.; Fukuda, M.; Takeda, N.; Niida, H.; Kato, H.; Shinkai, Y. G9a histone methyltransferase plays a dominant role in euchromatic histone H3 lysine 9 methylation and is essential for early embryogenesis. *Genes Dev.* **2002**, *16*, 1779–1791.

(19) McGarvey, K. M.; Fahrner, J. A.; Greene, E.; Martens, J.; Jenuwein, T.; Baylin, S. B. Silenced tumor suppressor genes reactivated by DNA demethylation do not return to a fully euchromatic chromatin state. *Cancer Res.* **2006**, *66*, 3541–3549.

(20) Kondo, Y.; Shen, L.; Ahmed, S.; Boumber, Y.; Sekido, Y.; Haddad, B. R.; Issa, J. P. Downregulation of histone H3 lysine 9 methyltransferase G9a induces centrosome disruption and chromosome instability in cancer cells. *PLoS ONE* **2008**, *3*, e2037.

(21) Huang, J.; Dorsey, J.; Chuikov, S.; Zhang, X.; Jenuwein, T.; Reinberg, D.; Berger, S. L. G9a and GLP methylate lysine 373 in the tumor suppressor p53. *J. Biol. Chem.* **2010**, *285*, 9636–9641.

(22) Kubicek, S.; O'Sullivan, R. J.; August, E. M.; Hickey, E. R.; Zhang, Q.; Teodoro, M. L.; Rea, S.; Mechtler, K.; Kowalski, J. A.; Homon, C. A.; Kelly, T. A.; Jenuwein, T. Reversal of H3K9me2 by a small-molecule inhibitor for the G9a histone methyltransferase. *Mol. Cell* **2007**, *25*, 473–481.

(23) Shi, Y.; Do, J. T.; Desponts, C.; Hahm, H. S.; Scholer, H. R.; Ding, S. A combined chemical and genetic approach for the generation of induced pluripotent stem cells. *Cell Stem Cell* **2008**, *2*, 525–528.

(24) Shi, Y.; Desponts, C.; Do, J. T.; Hahm, H. S.; Scholer, H. R.; Ding, S. Induction of pluripotent stem cells from mouse embryonic fibroblasts by Oct4 and Klf4 with small-molecule compounds. *Cell Stem Cell* **2008**, *3*, 568–574.

(25) Greiner, D.; Bonaldi, T.; Eskeland, R.; Roemer, E.; Imhof, A. Identification of a specific inhibitor of the histone methyltransferase SU(VAR)3−9. *Nature Chem. Biol.* **2005**, *1*, 143–145.

(26) Cole, P. A. Chemical probes for histone-modifying enzymes. *Nature Chem. Biol.* **2008**, *4*, 590–597.

(27) Frye, S. V.; Heightman, T.; Jin, J. Targeting Methyl Lysine. *Annu. Rep. Med. Chem.* **2010**, in press, DOI: 10.1016/S0065-7743(10)45020-4.

(28) Frye, S. V. The art of the chemical probe. *Nature Chem. Biol.* **2010**, *6*, 159–161.

(29) Chang, Y.; Zhang, X.; Horton, J. R.; Upadhyay, A. K.; Spannhoff, A.; Liu, J.; Snyder, J. P.; Bedford, M. T.; Cheng, X. Structural basis for G9a-like protein lysine methyltransferase inhibition by BIX-01294. *Nature Struct. Mol. Biol.* **2009**, *16*, 312–317.

(30) Quinn, A. M.; Allali-Hassani, A.; Vedadi, M.; Simeonov, A. A chemiluminescence-based method for identification of histone lysine methyltransferase inhibitors. *Molecular BioSystems* **2010**, *6*, 782–788.

(31) Liu, F.; Chen, X.; Allali-Hassani, A.; Quinn, A. M.; Wasney, G. A.; Dong, A.; Barsyte, D.; Kozieradzki, I.; Senisterra, G.; Chau, I.; Siarheyeva, A.; Kireev, D. B.; Jadhav, A.; Herold, J. M.; Frye, S. V.; Arrowsmith, C. H.; Brown, P. J.; Simeonov, A.; Vedadi, M.; Jin, J. Discovery of a 2,4-diamino-7-aminoalkoxyquinazoline as a potent and selective inhibitor of histone lysine methyltransferase G9a. *J. Med. Chem.* **2009**, *52*, 7950–7953.

(32) Collazo, E.; Couture, J. F.; Bulfer, S.; Trievel, R. C. A coupled fluorescent assay for histone methyltransferases. *Anal. Biochem.* **2005**, *342*, 86–92.

(33) Prepared as a racemic mixture.

(34) Min, J.; Allali-Hassani, A.; Nady, N.; Qi, C.; Ouyang, H.; Liu, Y.; MacKenzie, F.; Vedadi, M.; Arrowsmith, C. H. L3MBTL1 recognition of mono- and dimethylated histones. *Nature Struct. Mol. Biol.* **2007**, *14*, 1229–1230.

(35) Wigle, T. J.; Provencher, L. M.; Norris, J. L.; Jin, J.; Brown, P. J.; Frye, S. V.; Janzen, W. P. Accessing Protein Methyltransferase and Demethylase Enzymology Using Microfluidic Capillary Electrophoresis. *Chemistry & Biology* **2010**, in press.

(36) Morrison, J. F. Kinetics of the reversible inhibition of enzyme-catalysed reactions by tight-binding inhibitors. *Biochim. Biophys. Acta* **1969**, *185*, 269–286.

(37) Williams, J. W.; Morrison, J. F. The kinetics of reversible tight-binding inhibition. *Methods Enzymol.* **1979**, *63*, 437–467.

(38) Sakurai, M.; Rose, N. R.; Schultz, L.; Quinn, A. M.; Jadhav, A.; Ng, S. S.; Oppermann, U.; Schofield, C. J.; Simeonov, A. A miniaturized screen for inhibitors of Jumonji histone demethylases. *Mol. Biosyst.* **2010**, *6*, 357–364.

(39) Niesen, F. H.; Berglund, H.; Vedadi, M. The use of differential scanning fluorimetry to detect ligand interactions that promote protein stability. *Nature Protoc.* **2007**, *2*, 2212–2221.

(40) Vedadi, M.; Niesen, F. H.; Allali-Hassani, A.; Fedorov, O. Y.; Finerty, P. J., Jr.; Wasney, G. A.; Yeung, R.; Arrowsmith, C.; Ball, L. J.; Berglund, H.; Hui, R.; Marsden, B. D.; Nordlund, P.; Sundstrom, M.; Weigelt, J.; Edwards, A. M. Chemical screening methods to identify ligands that promote protein stability, protein crystallization, and structure determination. *Proc. Natl. Acad. Sci. U.S.A.* **2006**, *103*, 15835–15840.

(41) Allali-Hassani, A.; Wasney, G. A.; Chau, I.; Hong, B. S.; Senisterra, G.; Loppnau, P.; Shi, Z.; Moult, J.; Edwards, A. M.; Arrowsmith, C. H.; Park, H. W.; Schapira, M.; Vedadi, M. A survey of proteins encoded by nonsynonymous single nucleotide polymorphisms reveals a significant fraction with altered stability and activity. *Biochem. J.* **2009**, *424*, 15–26.